The Abdus Salam
International Centre for Theoretical Physics

United Nations
Educational, Scientific and
Cultural Organization

IAEA
International Atomic Energy Agency

2052-19

Summer College on Plasma Physics

10 - 28 August 2009

Relativistic Laser-Plasma Interactions
Part I & II

Milos Skoric
National Institute for Fusion Science
Japan

Relativistic Laser-Plasma Interactions
I & II

Miloš M. Škorić

Department of Simulation Science
National Institute for Fusion Science
Graduate University of Advanced Studies
National Institutes of Natural Sciences
Toki-shi, Japan

Introduction to relativistic physics of plasmas

Ever since the much acclaimed paper of Akhiezer and Polovin [1956] plasma theorists have been attempting to comprehend complex dynamics related to the propagation of high and ultra-high intensity electromagnetic (EM) radiation through a plasma. This topic was successfully revisited a number of years later by Kaw and Dawson [1970] whose analysis threw more light on the propagation of coupled longitudinal-transverse waves of arbitrary intensity, for high phase velocity solved by Max and Perkins [1971] (early review, Shukla et al. [1986]). Due to rapid progresses in ultrahigh intensity lasers over last decades, based on the invention of the chirped pulse amplification (CPA) and advanced femtotsecond techniques, it has become possible to drive electrons with relativistic energy opening up new avenues of relativistic nonlinear optics and plasma physics The problem of relativistic laser-plasma interactions is of particular interest concerning the fast ignition concept, in present laser inertial confinement fusion. Moreover, the understanding of relativistic laser pulse evolution in a plasma is basic to many applications, including optical-field-ionized x-ray lasers, plasma based electron accelerator schemes, also, as well as, the interpretation of some astrophysical phenomena (Mourou, 2007 and references, therein). Currently, the wide field of relativistic laser matter interaction has been diverging in two main broad directions; the first, related to laser fusion, high energy densities and laboratory astrophysics, and the second, related to ultra high field science, high energy particle acceleration and photon beam and ultra-fast attosecond phenomena. Many of these applications require stable channel guiding of intense laser beams over longer distances without significant energy losses. The pioneer papers in this field, did not consider the stability of the relativistic-wave solutions, related to nonlinear interaction between normal plasma modes. However, in a highly nonlinear system we have to deal with a number nonlinearly coupled modes under various plasma conditions. In this tutorial lecture we shall briefly address some of fundamental relativistic-plasma effects and implications.

http://www.nifs.ac.jp/report/nifs-proc74.html; Skoric, 2008

- Introduction
- Development of ultra-short pulse high-intensity lasers
- Free electron in ultra strong EM field
- Collective relativistic -plasma interaction

Relativistic Plasma Physics

- *Relativistic change of plasma index of refraction*
- *Ponderomotive force*
- *Induced Transparency*
- *Self-focusing of a laser beam*
- *Relativistic electronic parametric instabilities*
- *Complexity in Stimulated Raman back-Scattering (SRS)*
- *Stimulated: Raman and Electron acoustic backscatter*
- *SRS Cascade into Photon Condensation*
- *Relativistic EM localized structures- Solitons*

- Applications, various – Fast Ignition scheme in laser fusion
- Summary

Evolution of high-power laser systems

- 1960: Discovery of laser "a *solution* looking for a *problem*"
- 1960-1965: "Q-switched" & "mode-locked" lasers, intensity ~ 10^{12} W/cm^2
- 1965-1985: Increase in laser intensity ~ 10^{15} W/cm^2
- 1985: Discovery of CPA laser
- 1985-2008: up to (Ultra-) Relativistic intensity ~ 10^{24} W/cm^2

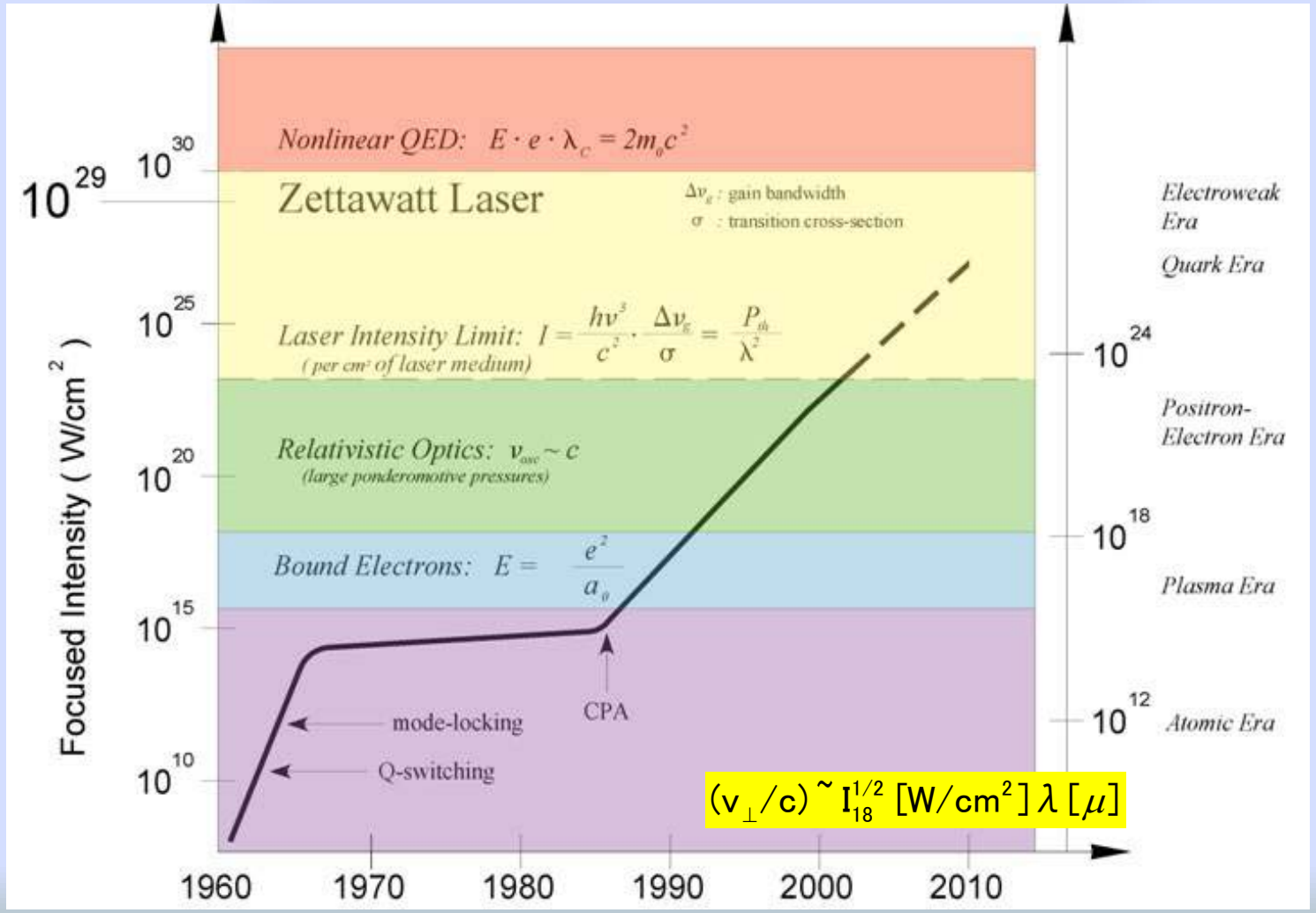

Pulse (Picosec) –> Expansion (x 1000) – Amplification – Compression -> Ultra-short pulse

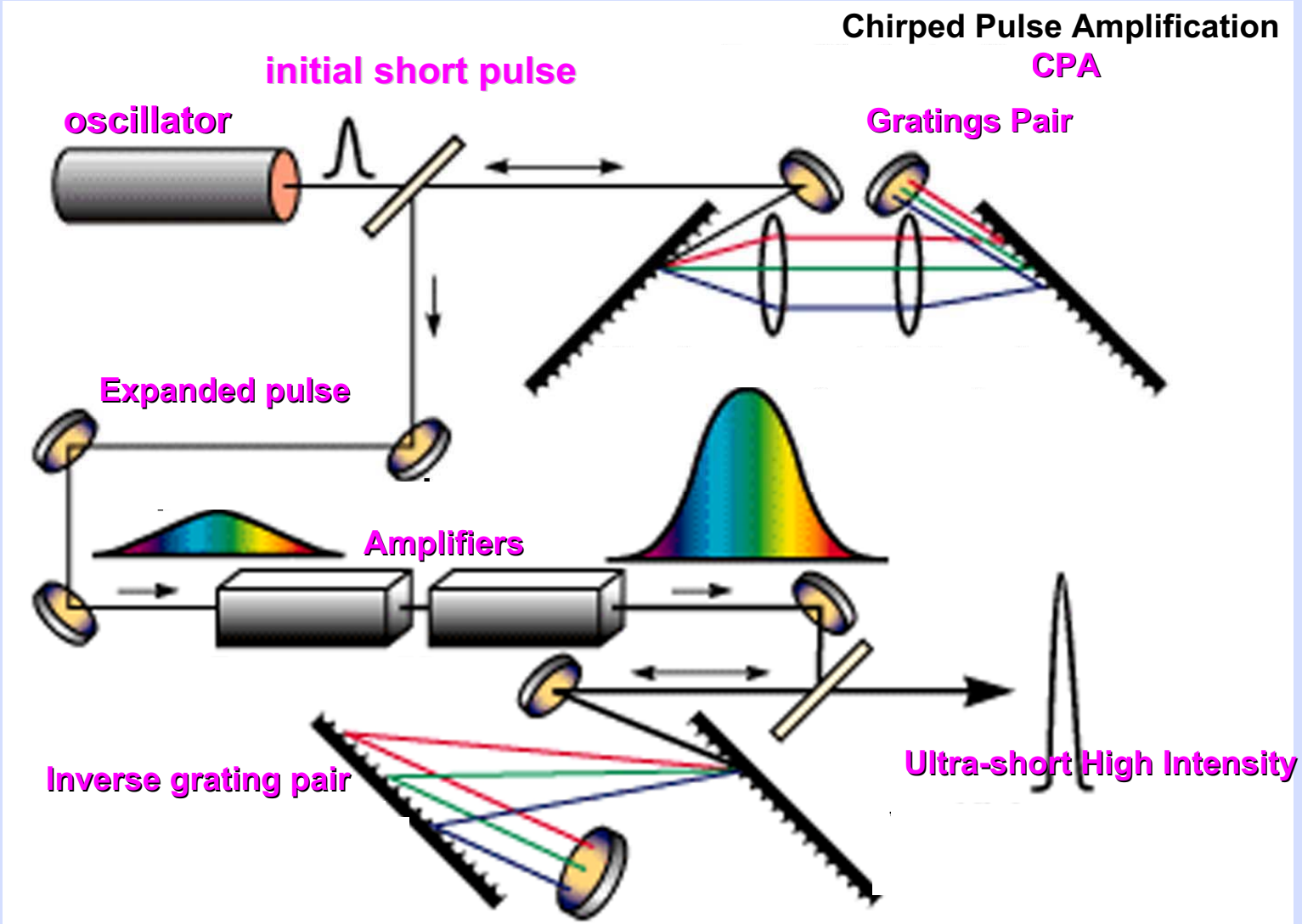

Concept of high-power ultra-short CPA laser

T- cube (T^3) – TableTop Terawatt - compact CPA laser (sub- picosec)

Free electron in a intense Electromagnetic (EM) field

Assumption: Free electron initially at rest interacts with intense, e.g. linearly- polarized plane EMW which propagates along x-axis

Relativistic equation of electron motion:

nonlinear

$$\frac{d\vec{p}}{dt} = -e(\vec{E} + \vec{v}_c \times \vec{B})$$

$$\vec{p} = m_e \gamma \vec{v}$$

$$\vec{E} = -\frac{\partial \vec{A}}{\partial t}$$

$$\vec{B} = \nabla \times \vec{A}$$

$$\gamma = \frac{1}{\sqrt{1 - v^2/c^2}} = \sqrt{1 + \frac{p^2}{m_e c^2}}$$

$$\nabla \cdot \vec{A} = 0$$

Coulomb gauge

$$\frac{d}{dt}(\vec{p} - e\vec{A}) = -e(\nabla \vec{A}) \cdot \vec{v}$$

Energy balance:

$$\frac{d}{dt}\gamma m_e c^2 = e\vec{v} \cdot \frac{\partial \vec{A}}{\partial t}$$

Relations:

$$\vec{p}_\perp = e\vec{A}$$

$$\vec{v}_\perp = \frac{e\vec{A}}{m_e \gamma}$$

Result:

$$\frac{p_x}{m_e c} = \frac{1}{2}\left(\frac{\vec{p}_\perp}{m_e c}\right)^2 \qquad \tan\theta = \left(\frac{2}{\gamma - 1}\right)^{1/2}$$

Longitudinal electron velocity component !!

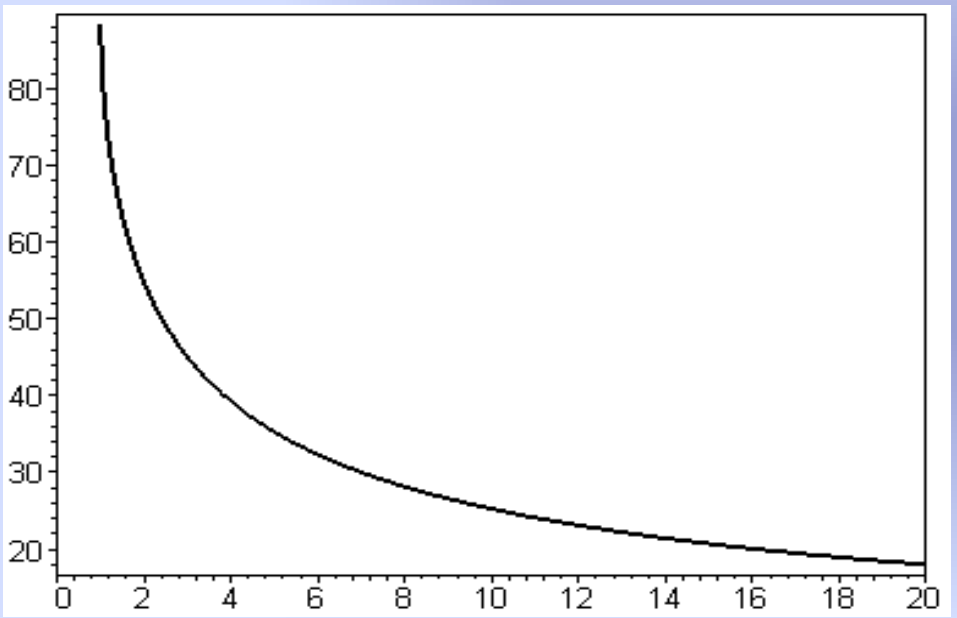

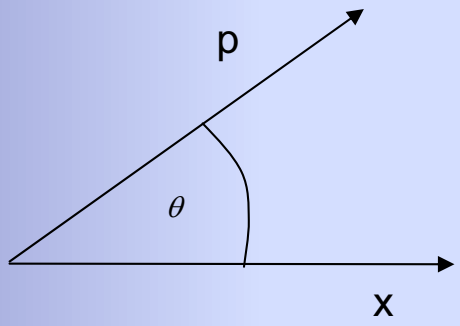

Trajectory of relativistic electrons in linearly- polarized EM wave

a) Laboratory frame

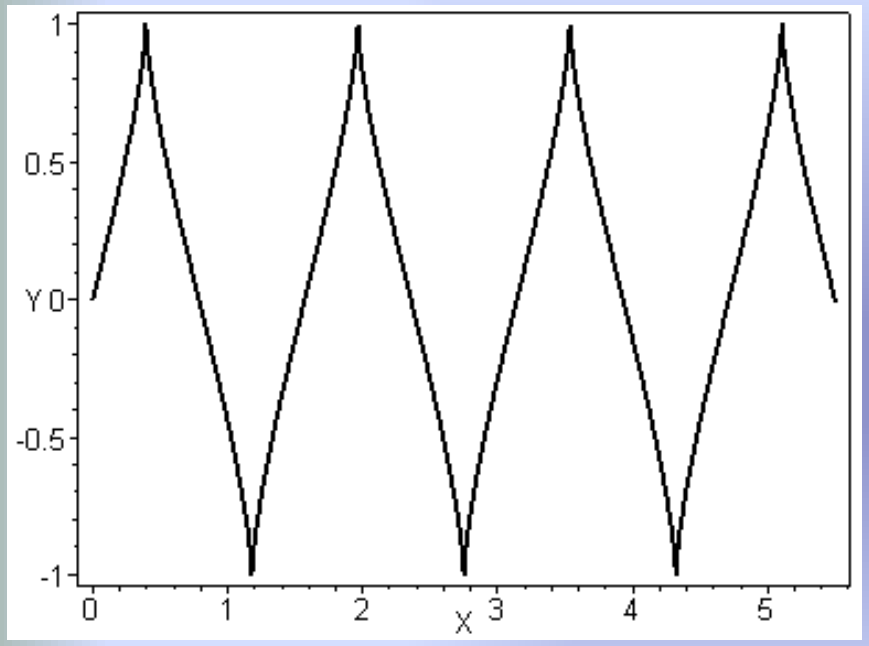

b) Moving frame with e- drift speed

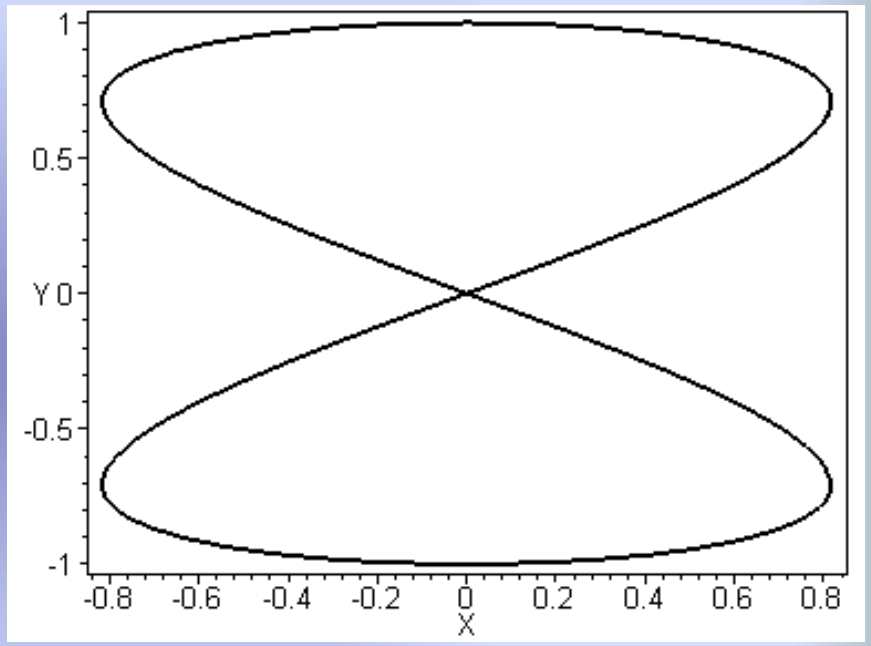

Trajectory of relativistic electrons in circularly polarized EM field:
a) Spiral – Lab frame b) Circular – Moving frame

Relativistic collective effects in laser-plasma interaction

CPA enables compact multi-TW up to beyond PW laser systems
Intensity at focus, in range 10^{17}-10^{24} W/cm^2 (moderate to ultra-relativistic electrons)
Propagation and channeling of relativistic short Laser- pulses in plasmas

Fast-Ignition concept (Inertial Confinement Laser- Fusion)

Applications

Novel Light Sources
X- Lasers (X-ray)
Higher harmonics generation
Laser-plasma particle Accelerators
Energetic ion and electron sources
Attosecond light sources
Laboratory Astrophysics

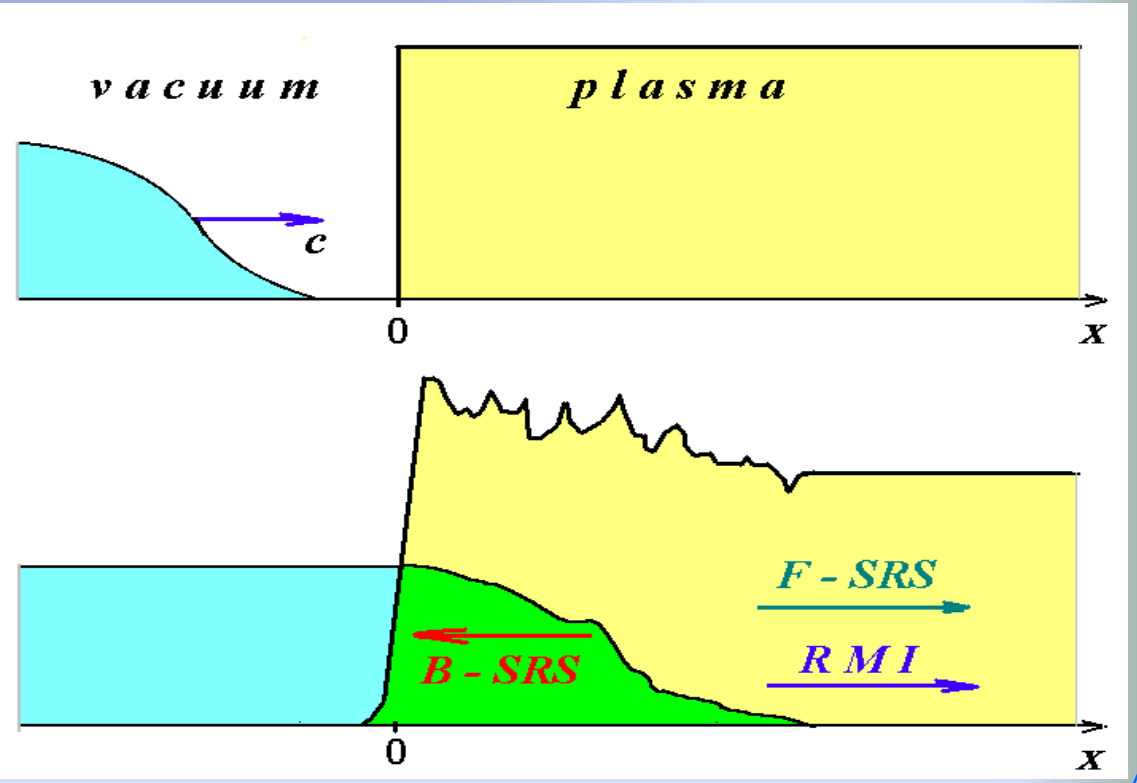

Basic relativistic effects in strongly nonlinear laser- plasma interaction

Relativistic change of plasma index of refraction

Basic equations:

$$\Delta\vec{A} - \frac{1}{c^2}\frac{\partial^2\vec{A}}{\partial t^2} = -\mu_0\vec{J}_\perp$$

$$\Delta\Phi = -\frac{\rho}{\varepsilon_0}$$

$$\frac{d}{dt}(\vec{p} - e\vec{A}) = -e[\nabla\Phi - (\nabla\vec{A})\cdot\vec{v}]$$

Dispersion relation for EMW:

$$\omega^2 = \frac{\omega_{pe}^2}{\gamma} + k^2c^2$$

$$\omega^2 > \frac{\omega_{pe}^2}{\gamma}$$

$$n_e < \gamma n_c$$

Index of refraction:

$$N^2 = 1 - \frac{\omega_{pe}^2}{\gamma\omega^2}$$

REAL

Relativistic transparency
EMW propagation in a plasma:

$$n_c < n_e < \gamma n_c$$

Relativistically Induced Transparency

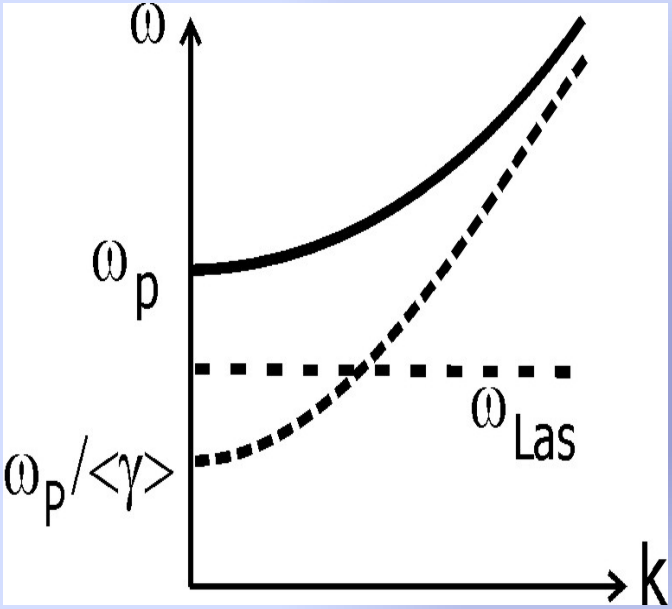

Light of frequency ω propagates through a plasma according to the well-known EM dispersion relation

$$\omega_0^2 = \omega_{p0}^2 / \langle \gamma \rangle + k^2 c^2$$

It depends on the plasma frequency $\omega_{p0}^2 = 4\pi e^2 n_e / m_0$ and the average $\langle \gamma \rangle$-factor. In overdense plasma with $\omega_0 < \omega_p$, light cannot propagate and is reflected from the surface. However, at relativistic intensities generating large $\langle \gamma \rangle$ -factor, the plasma becomes transparent; so called relativistic induced transparency

Ponderomotive force

- Circular polarized EM wave
- 1D cold plasma

$$f_{nl} = -\frac{e^2}{2\gamma m_e}\frac{\partial A^2}{\partial x}$$

Relativistic effects "reduce" the strenght of ponderomotive force by factor of γ

Radiation pressure $$P_{rad} = (1+R)\frac{I}{c}$$

R – Reflection coefficient
I – intensity

For laser beam intensity of 10^{22} W/cm^2
Radiation pressure is larger than 100 Gbar

Relativistic Pulse Profile Steepening

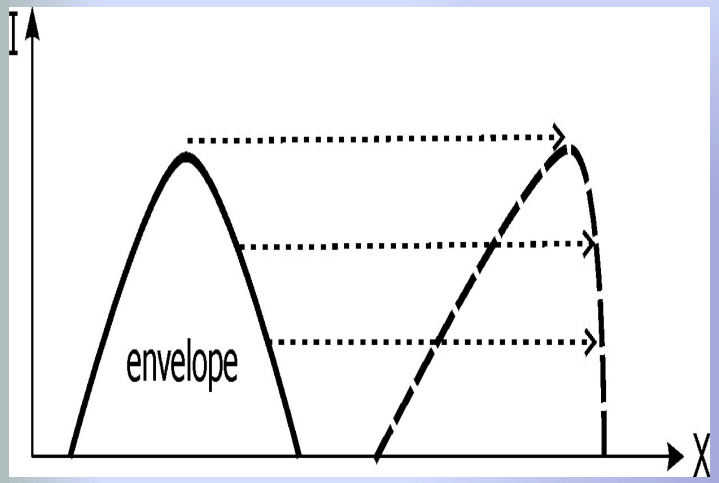

Another important effect is the **steepening** of pulse envelopes propagating with group velocity $v_{gr}=cn$. The peak region with high intensity runs faster than those with low intensity at the pulse head, and this leads to optical shock formation. Pulse shapes with steeply rising fronts are interesting for studying high intensity effects in matter.

Self-focusing of a laser beam

Change of index of refraction + ponderomotive force

Laser beam intensity is largest at the center and decreases in radial direction

$$\frac{dI(r)}{dr} < 0$$

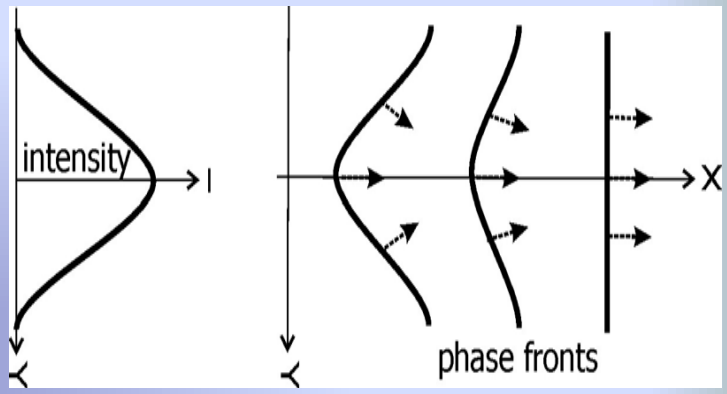

Ponderomototive force pushes away electrons from the Max- intensity region

$$\frac{d\omega_{pe}(r)}{dr} > 0$$

$v_{ph}=c/n$

Optical lense effect

Index of refraction

$$N^2(r) = 1 - \frac{\omega_{pe}^2(r)}{\gamma(r)\omega^2} \quad \Rightarrow \quad \frac{dN(r)}{dr} < 0$$

Competition: Dispersion – Self-focusing

Threshold: $P_c(GW) = 1.62\ \omega^2 / \omega_{pe}^2$

Self-focusing and filamentation of a laser beam

Change of index of refraction + ponderomotive force

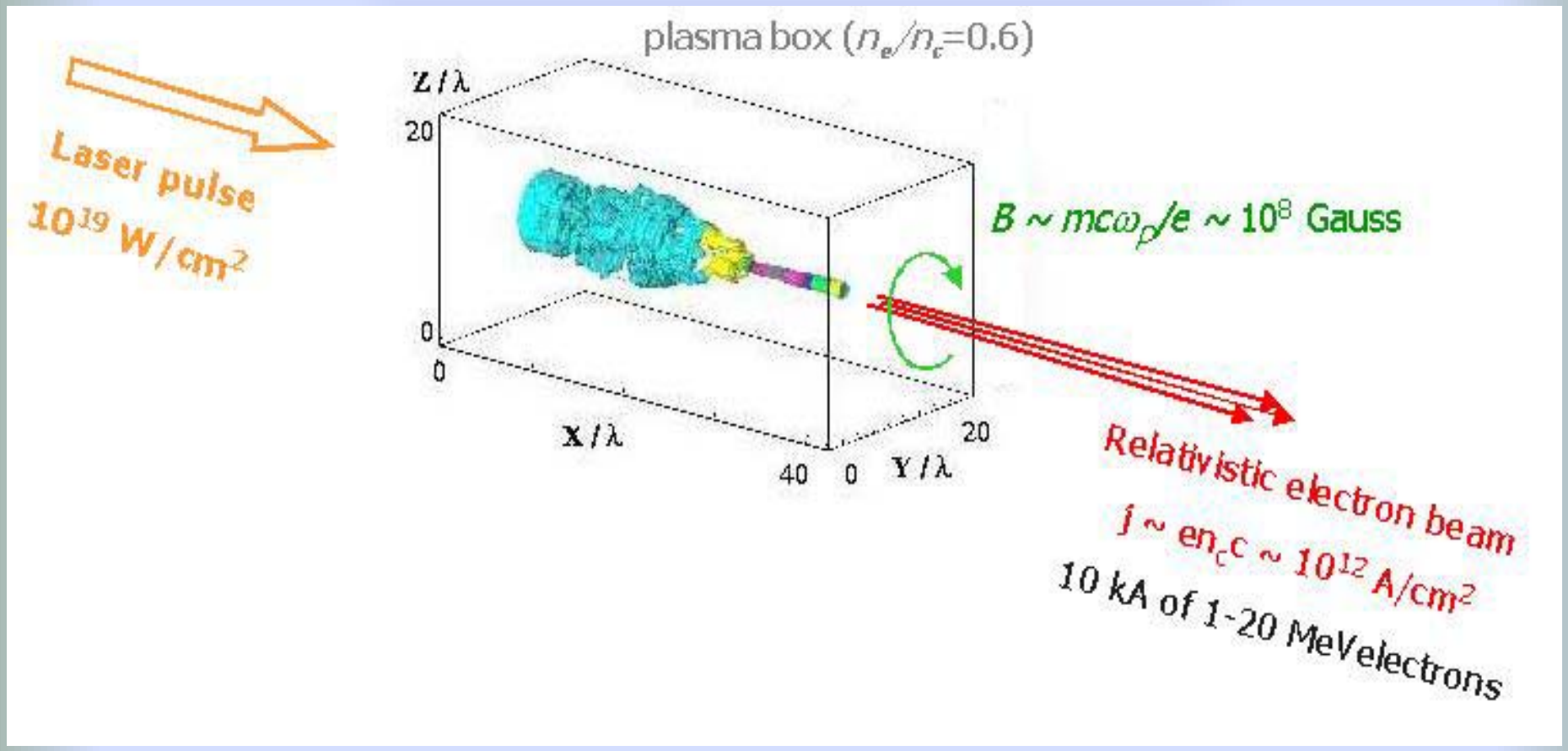

After, Pukhov et al.

Electronic Parametric Wave Coupling

Many instabilities in plasma can be classified as a parametric excitation of resonantly coupled waves; a multi-wave process, as externally driven laser pump wave can interact with a spectrum of waves. Still, often it can be well described as three wave interaction (3WI) as long as certain resonant triplet evolves (almost) independently of the others. The 3WI is the lowest-order nonlinear effect for a system approximated by a linear superposition of discrete coherent waves. For the 3WI to occur, wave frequencies and wave vectors must satisfy matching condition.

$$\omega_- = \omega_0 - \omega_1, \qquad \mathbf{k}_- = \mathbf{k}_0 - \mathbf{k}_1,$$

$$\omega_+ = \omega_0 + \omega_1, \qquad \mathbf{k}_+ = \mathbf{k}_0 + \mathbf{k}_1,$$

where modes ”0” and ”1” represent laser pump and plasma waves and mode ”-” and “+” represent scattered waves (Stokes/ anti-Stokes wave).

Skoric, Lecture Notes, NIFS-Proc no74 (2008)
http://www.nifs.ac.jp/report/nifs-proc74.html

There is a rich experimental and theoretical evidence in laboratory & space plasmas for nonlinear 3WIs that involve EM waves, Langmuir waves and ion-acoustic waves. The 3WI decay schemes, in particular in laser plasmas:

(i) photon ➔ photon + plasmon (Langmuir)–stimulated Raman scattering *SRS*

(ii) photon ➔ photon + ion-acoustic wave – stimulated Brillouin scattering *SBS*

(iii)photon ➔ two plasmons - Two plasmon decay instability *TPD*

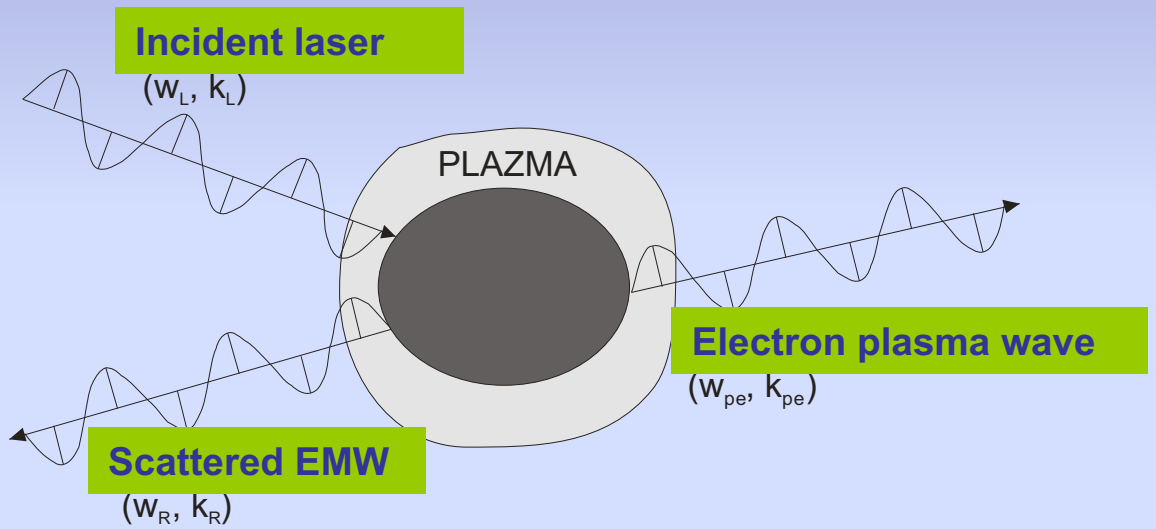

Schematics of stimulated Raman scattering

Electron and ion parametric instabilities

Laser light EMW decays during plasma interaction into excited plasma and EM modes

Electronic plasma wave modes:
- **Stimulated Raman scattering-**
- **Two-plasmon decay-**

Ion plasma wave modes:
- **Stimulated Brillouin scattering**
- **Ion-acoustic decay**

Matching conditions: $\omega_L = \omega_r + \omega_p, \quad \vec{k}_L = \vec{k}_r + \vec{k}_p$

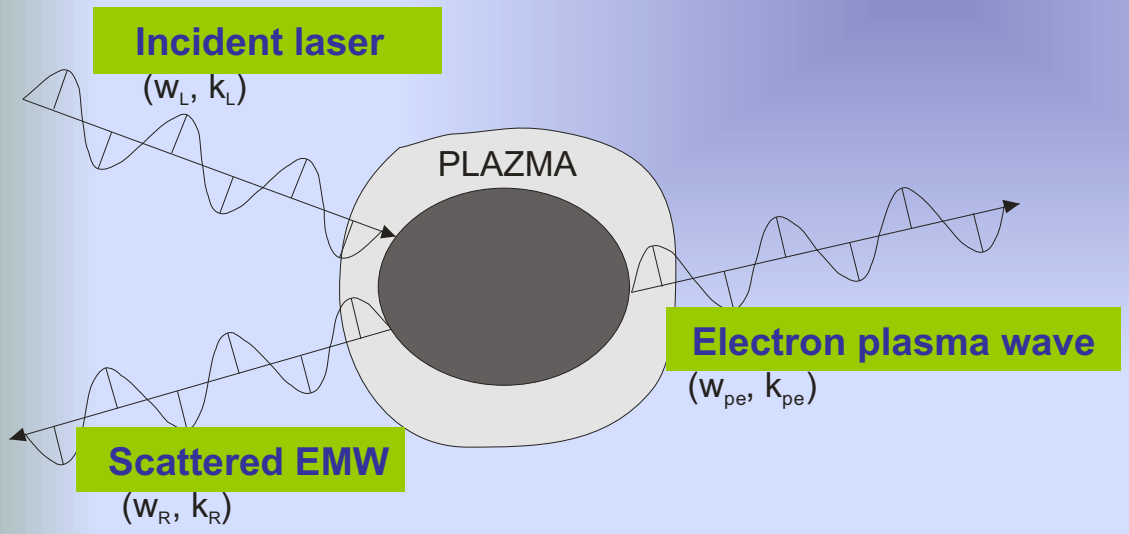

Schematics of Raman instability

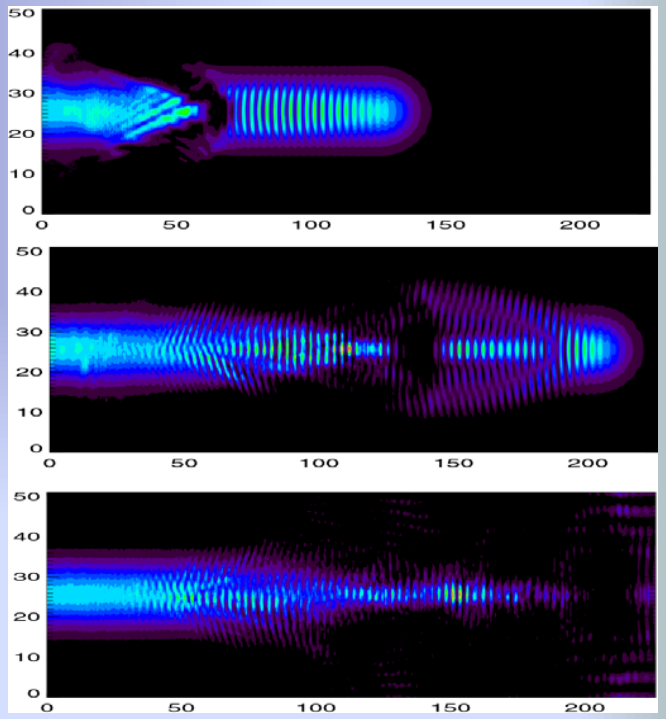

Destruction of *2D laser beam front*

Some important parametric decay mechanisms for laser plasmas

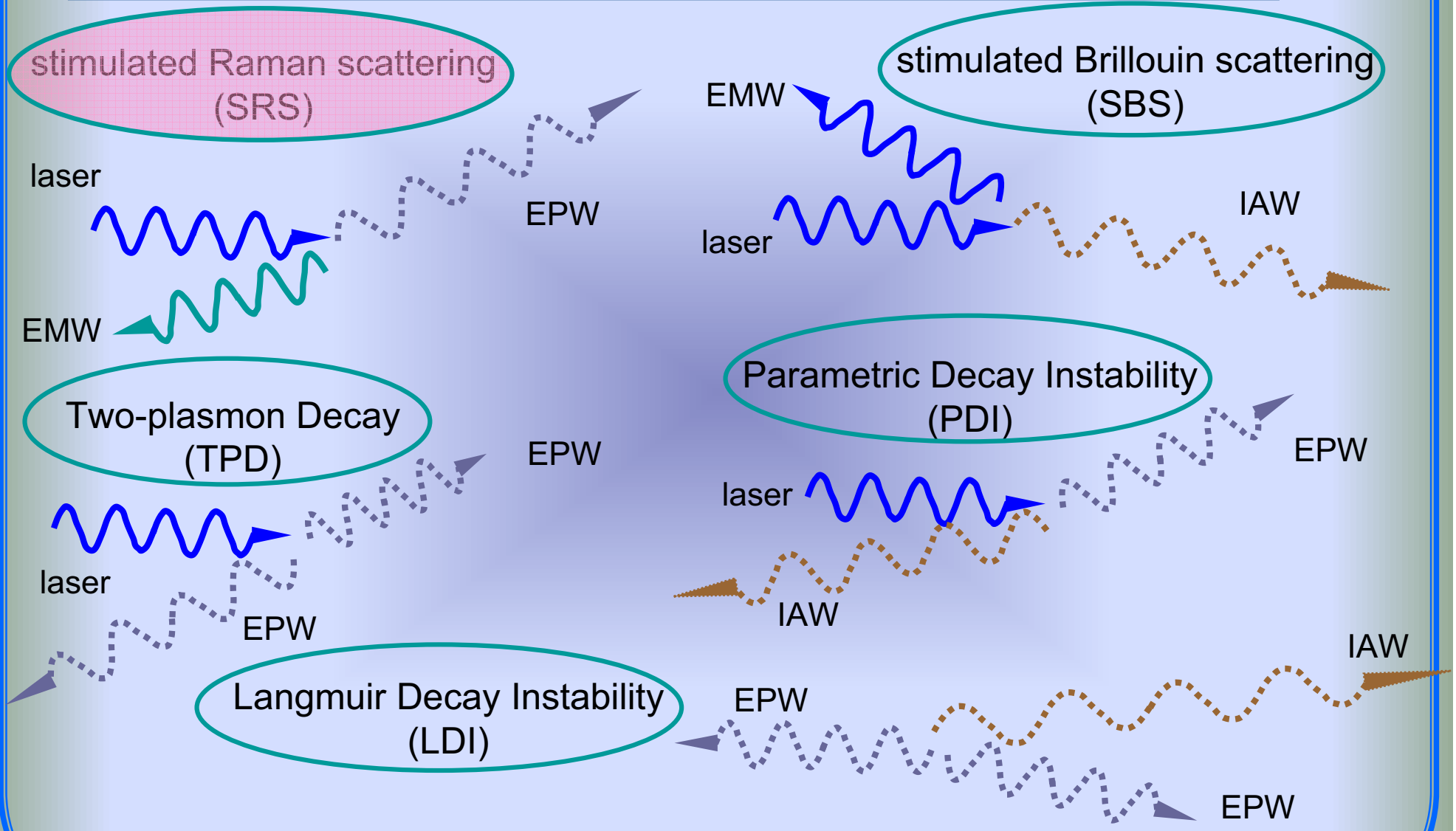

after D. Montgomery (LANL) PRL2002

Stimulated Raman Scattering (SRS)

The stimulated Raman scattering is a parametric decay of an incident EM wave into a scattered light and an electron plasma (EPW- Langmuir) wave. The matching condition for the frequencies and wave numbers are

$$\omega_0 = \omega_s + \omega_{EPW}, \qquad k_0 = \pm k_s + k_{EPW},$$

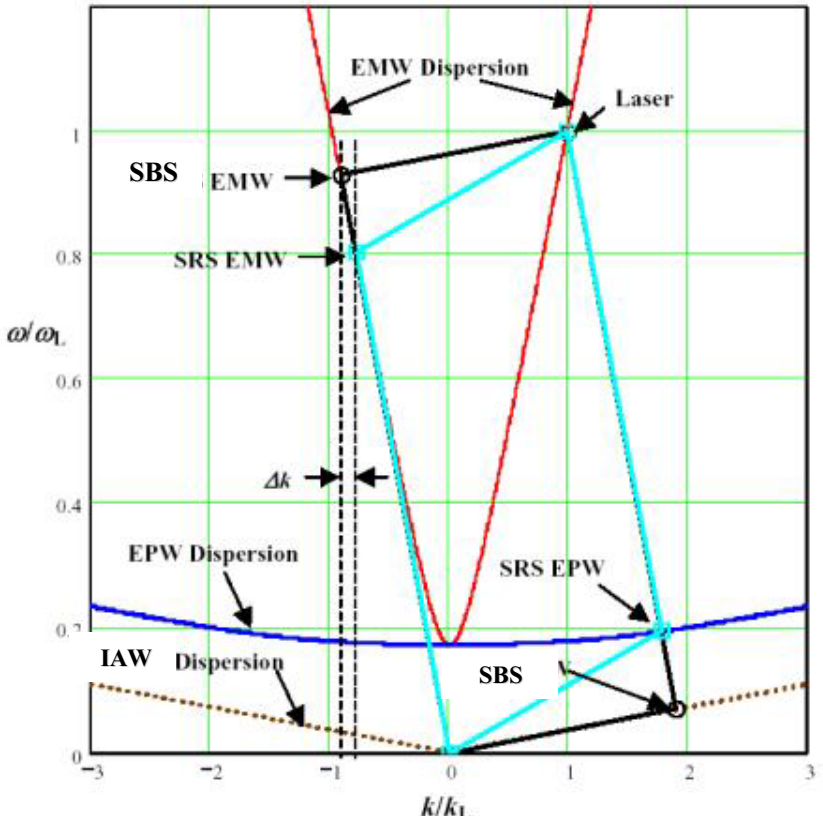

Analogous process to SRS, however, involving EMW scattering on an ion acoustic wave (IAW) : stimulated Brillouin scattering (SBS) instability

SRS matching condition

$$k_0 = \frac{\omega_0}{c}\left(1 - \frac{n}{n_{cr}}\right)^{1/2},$$

$$k_s = \frac{\omega_s}{c}\left(1 - \frac{\omega_p^2}{\omega_s^2}\right)^{1/2},$$

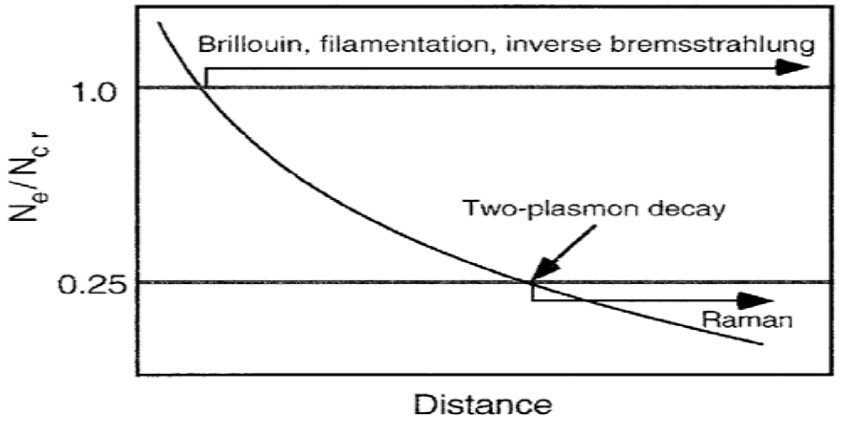

Stimulated Raman/ Compton Scattering (SRS)

The stimulated Raman scattering is a parametric decay of an incident EM wave into a scattered light and an electron plasma (EPW- Langmuir) wave. The matching condition for the frequencies and wave numbers are

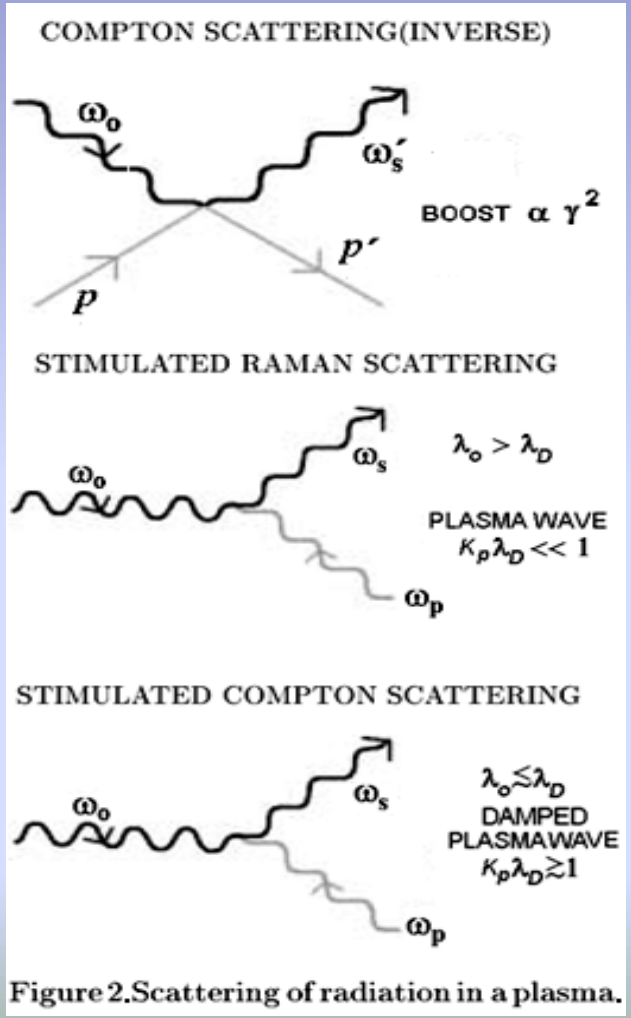

Figure 2.Scattering of radiation in a plasma.

$$\omega_0 = \omega_s + \omega_{EPW}, \qquad k_0 = \pm k_s + k_{EPW},$$

SRS matching condition

$$k_0 = \frac{\omega_0}{c}\left(1 - \frac{n}{n_{cr}}\right)^{1/2},$$

$$k_s = \frac{\omega_s}{c}\left(1 - \frac{\omega_p^2}{\omega_s^2}\right)^{1/2},$$

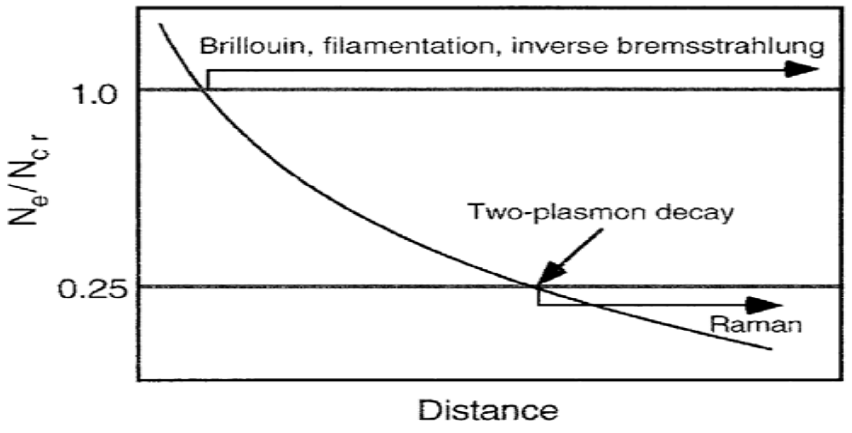

Relativistic electronic parametric instabilities

For relativistic parametric instabilities in cold electron plasma with fixed ions we assume a linearly polarized laser pump (vector potential- **A**)

$$\mathbf{A}_0 = \frac{1}{2} A_0 \mathbf{e}_y e^{i(\mathbf{k}_0 \cdot \mathbf{x} - \omega_0 t)} + c.c.$$

and two daughter waves

$$\mathbf{A}_+ = \frac{1}{2} A_+ \mathbf{e}_y e^{i(\mathbf{k} \cdot \mathbf{x} - \omega t)} e^{i(\mathbf{k}_0 \cdot \mathbf{x} - \omega_0 t)} + c.c.$$

$$\mathbf{A}_- = \frac{1}{2} A_- \mathbf{e}_y e^{-i(\mathbf{k} \cdot \mathbf{x} - \omega^* t)} e^{i(\mathbf{k}_0 \cdot \mathbf{x} - \omega_0 t)} + c.c.$$

$$\mathbf{E} = -\nabla\phi - \frac{\partial \mathbf{A}}{\partial t},$$

$$\mathbf{B} = \nabla \times \mathbf{A},$$

$$\nabla \times \mathbf{B} = \mu_0 \mathbf{j} + \varepsilon_0 \mu_0 \frac{\partial \mathbf{E}}{\partial t},$$

$$\frac{\partial n}{\partial t} + \nabla \cdot (n\mathbf{v}) = 0,$$

$$m \frac{d\gamma \mathbf{v}}{dt} = -e(\mathbf{E} + \mathbf{v} \times \mathbf{B}),$$

$\mathbf{v}$ is the velocity and $\gamma = \left(1 - v^2/c^2\right)^{-1/2}$, is the relativistic Lorentz factor.

Maxwell equations **Relativistic e-fluid equations**

Basic dynamical equations

The relativistic wave equation and the cold electron momentum equation, in terms of vector and scalar potential ($\boldsymbol{A}$ and ϕ, respectively), in the *Coulomb* (radiation) gauge, where $\boldsymbol{\nabla} \cdot \boldsymbol{A} = 0$, are written as (e.g. Jackson, 1975)

$$\nabla^2 \boldsymbol{A} - \frac{1}{c^2}\frac{\partial^2}{\partial t^2}\boldsymbol{A} = -\frac{4\pi}{c}\boldsymbol{J}_\perp, \tag{4.53}$$

where $\boldsymbol{J}_\perp$ is the transverse component of the total electron current $\boldsymbol{J} = \boldsymbol{J}_\perp + \boldsymbol{J}_{\shortparallel} = en\boldsymbol{v}$, where n is the electron density and ions assumed to be fixed, and

$$\frac{\partial \boldsymbol{p}}{\partial t} + (\boldsymbol{v}\boldsymbol{\nabla})\,\boldsymbol{p} = e\boldsymbol{\nabla}\phi + \frac{e}{c}\frac{\partial}{\partial t}\boldsymbol{A} - \frac{e}{c}\boldsymbol{v} \times (\boldsymbol{\nabla} \times \boldsymbol{A})\,, \tag{4.54}$$

where $\boldsymbol{p} = \gamma m\boldsymbol{v}$, is the electron momentum, $\boldsymbol{v}$, is the electron velocity and $\gamma = (1 + p^2/m^2c^2$ is the relativistic Lorentz factor. The relativistic electron momentum equation can be transformed by using the vector identity which after a straightforward algebra gives

$$\frac{\partial}{\partial t}\left(\boldsymbol{p} - \frac{e}{c}\boldsymbol{A}\right) = e\boldsymbol{\nabla}\phi - mc^2\boldsymbol{\nabla}\gamma + \boldsymbol{v} \times \left[\boldsymbol{\nabla} \times \left(\boldsymbol{p} - \frac{e}{c}\boldsymbol{A}\right)\right], \tag{4.55}$$

that is the equation for the generalized momentum $\left(\boldsymbol{p} - \frac{e}{c}\boldsymbol{A}\right)$. By taking the ***curl*** of the above relation, one can readily conclude that if $\boldsymbol{\nabla} \times \left(\boldsymbol{p} - \frac{e}{c}\boldsymbol{A}\right)$ is equal to zero initially, it will remain zero at later times. Therefore, an important relation, $\boldsymbol{p}_\perp = \frac{e}{c}\boldsymbol{A}$, is found, which after a substitution in $\boldsymbol{J}_{\shortparallel}$, simplifies the wave equation in terms of the vector potential $\boldsymbol{A}$, (McKinstrie & DuBois, PF 1988)

Using vector identity $\nabla \times (\nabla \times \mathbf{A}) = \nabla(\nabla \cdot \mathbf{A}) - \nabla^2 \mathbf{A}$

from Maxwell equations one obtains

$$\frac{1}{c^2}\frac{\partial^2 \mathbf{A}}{\partial t^2} - \nabla^2 \mathbf{A} + \nabla\left(\frac{1}{c^2}\frac{\partial \phi}{\partial t} + \nabla \cdot \mathbf{A}\right) = \mu_0 \mathbf{j},$$

On the other hand, the equation of motion can be rewritten, as

$$\frac{\partial \gamma \mathbf{v}}{\partial t} = \frac{e}{m}\left(\nabla\phi + \frac{\partial \mathbf{A}}{\partial t}\right) - c^2 \nabla\gamma.$$

Ponderomotive force

Further, eqs. are analyzed order by order expansion in the laser amplitude

$$\mathbf{j} = -en\mathbf{v} = \mathbf{j}^{[1]} + \mathbf{j}^{[2]} + \mathbf{j}^{[3]} + \ldots$$

$$\mathbf{j}^{[1]} = -en_0\mathbf{v}^{[1]},$$
$$\mathbf{j}^{[2]} = -en_0(\mathbf{v}^{[2]} + n^{[1]}\mathbf{v}^{[1]}),$$
$$\mathbf{j}^{[3]} = -en_0(\mathbf{v}^{[3]} + n^{[1]}\mathbf{v}^{[2]} + n^{[2]}\mathbf{v}^{[1]}),$$

$$\gamma \approx 1 + \frac{1}{2}\frac{v^2}{c^2} + \ldots = 1 + \frac{1}{2}\frac{(\mathbf{v}_0 + \mathbf{v}_+ + \mathbf{v}_-)^2}{c^2} + \ldots$$

For the scattered waves, on the other hand, we have

$$\mathcal{D}_+ A_+ = \Gamma \mathcal{D}_1^+ A_+ - \Gamma \mathcal{D}_2 A_-^*,$$

$$\mathcal{D}_- A_-^* = \Gamma \mathcal{D}_1^- A_-^* - \Gamma \mathcal{D}_2 A_+,$$

where $\Gamma = \frac{\omega_p^2 \beta^2}{4}$ and $\mathcal{D}_\pm = \left[(\omega \pm \omega_0)^2 - \omega_p^2 - c^2(k \pm k_0)^2\right],$

$$\mathcal{D}_1^\pm = \left(\frac{c^2 k^2}{\omega^2 - \omega_p^2} + \frac{c^2(k \pm 2k_0)^2}{(\omega \pm 2\omega_0)^2 - \omega_p^2} - 3 \right),$$

$$\mathcal{D}_2 = \left(\frac{c^2 k^2}{\omega^2 - \omega_p^2} + \frac{2c^2 k_0^2}{4\omega_0^2 - \omega_p^2} - \frac{3}{2} \right).$$

Finally combined, we get hybrid dispersion relation

$$\mathcal{D}_- \mathcal{D}_+ = \Gamma(\mathcal{D}_- \mathcal{D}_1^+ + \mathcal{D}_+ \mathcal{D}_1^-) + \Gamma^2(\mathcal{D}_2^2 - \mathcal{D}_1^+ \mathcal{D}_1^-).$$

term $\sim \Gamma^2$ can be neglected.

which is complicated a sixth order equation in ω .

Forward-SRS
Backward-SRS
Rel. Modulational Instability

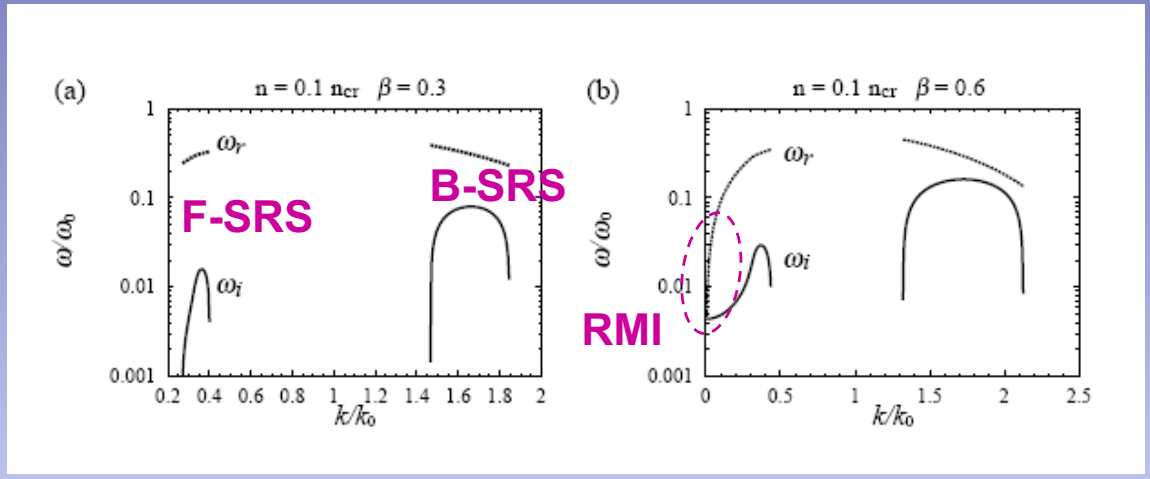

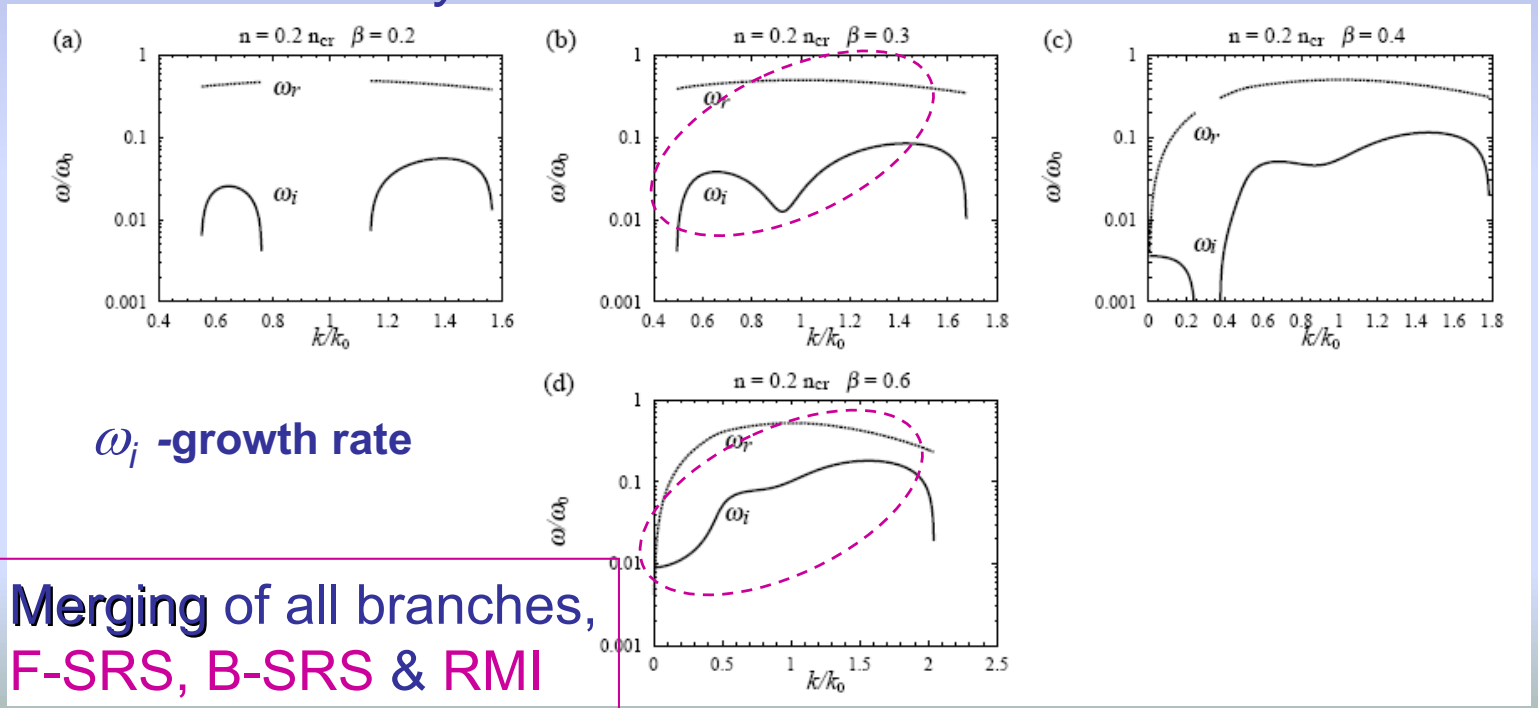

ω_i **-growth rate**

Merging of all branches,
F-SRS, B-SRS & RMI

Complexity in relativistic plasma interactions

Complex phenomena in relativistic plasma interactions

Inhibition of electric fields
Transport and collimation of electron beams
Energy deposition and target heating
Return electron current

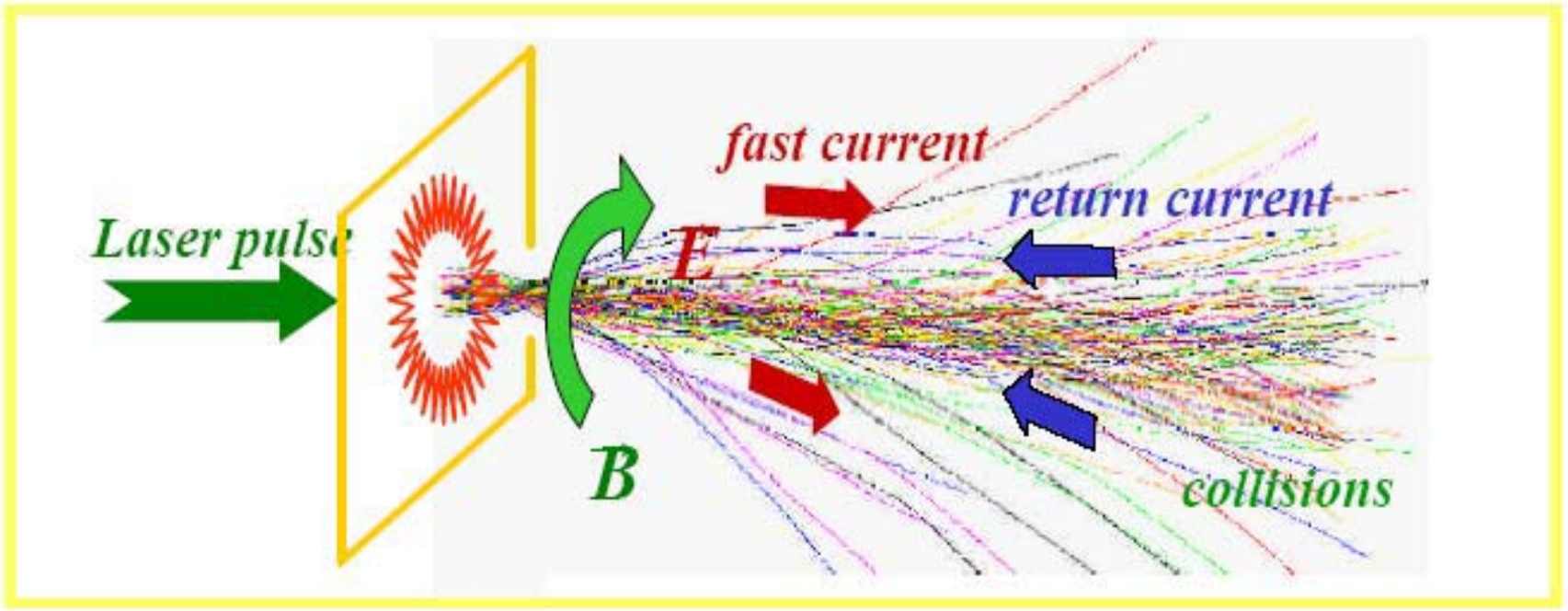

Charge separation effects
Induced (E, B) fields, wave turbulence, return currents, focusing , beam control
Instabilities: self-focusing, filamentation- coalescence, Weibel instabilities

Transition to Chaos in relativistic backward SRS

The one-dimensional model of SRS, assumes a uniform plasma layer of thickness L, irradiated by a laser beam from $x < 0$, which enters the plasma at $x \geq 0$, boundary.. The EPW and the scattered light are allowed to grow from their thermal noise levels (ε_1 and ε_2, respectively). Moreover, the EPW is subjected to a weak dissipation characterized by the linear damping rate v_e. The nonlinear 3WI model derived here for the case of SRS describes the spatiotemporal evolution of complex amplitudes of the pump (a_0), scattered (a_1) and EPW (a_2) in a weakly coupling approximation. These equations are obtained from Maxwell's and fluid vlasma eauations in WKB approximation, assuming the resonant matching between frequencies and wave numbers of three waves ($\omega_0 = \omega_1 + \omega_2, \mathbf{k}_0 = \mathbf{k}_1 + \mathbf{k}_2$) closely satisfying the corresponding linear dispersion relations

$$\omega_{0,1}^2 = \omega_{pe}^2 + k_{0,1}^2 c^2, \ \omega_2^2 = \omega_{pe}^2 + 3k_2^2 v_{te}^2, \tag{3.34}$$

where indices 0, 1, and 2 stand for the pump, scattered, and EPW, respectively; ω_{pe} for electron plasma frequency; and v_{te} for electron thermal velocity. For the case of *backscattering*, which is of most practical importance, the corresponding set of 3WI equations reads [102]

$$\begin{aligned}
\frac{\partial a_0}{\partial \tau} + V_0 \frac{\partial a_0}{\partial \xi} &= -a_1 a_2, \\
\frac{\partial a_1}{\partial \tau} - V_1 \frac{\partial a_1}{\partial \xi} &= a_0 a_2^*, \\
\frac{\partial a_2}{\partial \tau} + V_2 \frac{\partial a_2}{\partial \xi} &= \beta_0^2 a_0 a_1^* - \Gamma a_2 + i\delta \left|a_2\right|^2 a_2.,
\end{aligned} \tag{3.35}$$

nonlinear EPW

with time and space variables $\tau = \omega_0 t, \xi = x/L$, where the dimensionless amplitudes of the coupled waves are related to the physical quantities, electric fields E_0 and $E_1$of the two electromagnetic waves, and EPW-driven electron density fluctuation δn_e,

$$\beta_0 \equiv \frac{v_{osc}}{c} = \frac{e\mathcal{E}_0}{m_e \omega_0 c}$$

Laser pump strength

$$\delta = \frac{3\omega_0^2 \omega_1}{c^2 \omega_{pe} k_2^2}$$

Relativistic NL freq. shift

e.g. Rosenbluth et al. , 1971

Transition to Chaos in relativistic backward SRS

The one-dimensional model of SRS, assumes a uniform plasma layer of thickness L, irradiated by a laser beam from $x < 0$, which enters the plasma at $x \geq 0$, boundary.. The EPW and the scattered light are allowed to grow from their thermal noise levels (ε_1 and ε_2, respectively). Moreover, the EPW is subjected to a weak dissipation characterized by the linear damping rate v_e. The nonlinear 3WI model derived here for the case of SRS describes the spatiotemporal evolution of complex amplitudes of the pump (a_0), scattered (a_1) and EPW (a_2) in a weakly coupling approximation. These equations are obtained from Maxwell's and fluid vlasma eauations in WKB approximation, assuming the resonant matching between frequencies and wave numbers of three waves ($\omega_0 = \omega_1 + \omega_2, \mathbf{k}_0 = \mathbf{k}_1 + \mathbf{k}_2$) closely satisfying the corresponding linear dispersion relations

$$\omega_{0,1}^2 = \omega_{pe}^2 + k_{0,1}^2 c^2, \ \omega_2^2 = \omega_{pe}^2 + 3k_2^2 v_{te}^2, \tag{3.34}$$

where indices 0, 1, and 2 stand for the pump, scattered, and EPW, respectively; ω_{pe} for electron plasma frequency; and v_{te} for electron thermal velocity. For the case of *backscattering*, which is of most practical importance, the corresponding set of 3WI equations reads [102]

$$\begin{aligned}
\frac{\partial a_0}{\partial \tau} + V_0 \frac{\partial a_0}{\partial \xi} &= -a_1 a_2, \\
\frac{\partial a_1}{\partial \tau} - V_1 \frac{\partial a_1}{\partial \xi} &= a_0 a_2^*, \\
\frac{\partial a_2}{\partial \tau} + V_2 \frac{\partial a_2}{\partial \xi} &= \beta_0^2 a_0 a_1^*,
\end{aligned}$$

Elliptic function solution

Steady-state saturation

Standard 3WI model

with time and space variables $\tau = \omega_0 t, \xi = x/L$, where the dimensionless amplitudes of the coupled waves are related to the physical quantities, electric fields E_0 and $E_1$of the two electromagnetic waves, and EPW-driven electron density fluctuation δn_e,

$$\beta_0 \equiv \frac{v_{osc}}{c} = \frac{e\mathcal{E}_0}{m_e \omega_0 c}$$

Laser pump strength

e.g. Forslund PF , 1977

The most useful information on the SRS is contained in the reflectivity R, which designates a fraction of incident laser intensity reflected backward

$$R = \frac{V_0 \left|a_1(0)\right|^2}{V_1 \left|a_0(0)\right|^2} \tag{3.41}$$

with its maximum value normalized to unity in the stationary case. To solve (3.35), appropriate initial and boundary conditions are required. We choose physically realistic boundary conditions, while the choice of the plasma slab length satisfies the criterion for the occurrence of the absolute instability. The wave amplitudes obey the corresponding initial and nonzero source fixed boundary conditions,

$$\begin{aligned} a_0(x,0) &= 0 \quad (\text{for } x>0), a_0(0,t) = A_0 \\ a_1(x,0) &= a_1(L,t) = \varepsilon_1 A_0 \quad a_2(x,0) = a_2(x,t) = 0 \end{aligned} \tag{3.42}$$

where A_0 follows from (3.36) for $E_0(0) = \mathcal{E}_0$.
Analysis has shown that $V_1 V_2 > 0$, gives the convective instability, while for $V_1 V_2 < 0$, absolute instability appears, if the additional condition is satisfied, namely

$$\frac{\gamma_0^2 l^2}{|V_1 V_2|} > \frac{\pi^2}{4}.$$

$$\gamma_0 \approx 0.5\beta_0 \sqrt{\alpha/(1-\alpha)}\omega_0$$
$$\alpha = \omega_{pe}/\omega_0 = \sqrt{n/n_{cr}}$$

where γ_0 is the uniform linear parametric instability growth rate and l is the length of the system.

Bifurcations to low-dimensional Chaos in B-SRS

By varying the control (laser& plasma) parameters, Route to chaos in space-time in 3WI relativistic B-SRS is found : via steady-state, periodic, quasi-periodic and intermittent transition to chaos. Complexities in non-stationary bwd-Raman regimes include, strong spiky- burst like temporal Reflectivity & broadened blue-shifted incoherent spectra.

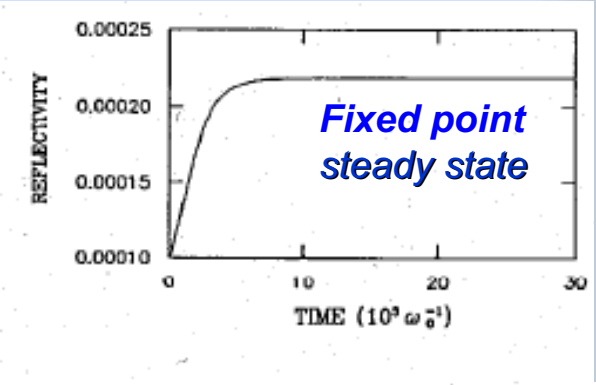

Figure 1:
Time evolution of the reflectivity of stimulated Raman backscattering for the parameters: $\mathbf{v_{osc} = 0.005\,c}$, $\nu_e = 10^{-8}\,\omega_{pe}$, $n_0 = 0.1\,n_{cr}$, $L = 100\,c/\omega_0$, $T_e = 1\,\mathrm{keV}$.

$$\frac{\partial a_0}{\partial \tau} + V_0 \frac{\partial a_0}{\partial \xi} = -a_1 a_2,$$

$$\frac{\partial a_1}{\partial \tau} - V_1 \frac{\partial a_1}{\partial \xi} = a_0 a_2^*,$$

$$\frac{\partial a_2}{\partial \tau} + V_2 \frac{\partial a_2}{\partial \xi} = \beta_0^2 a_0 a_1^* - \Gamma a_2 + i\delta \left|a_2\right|^2 a_2.,$$

with time and space variables $\tau = \omega_0 t, \xi = x/L$, where the dimensionless amplitudes of the coupled waves are related to the physical quantities, electric fields E_0 and $E_1$of the two electromagnetic waves, and EPW-driven electron density fluctuation δn_e,

laser

L -Under-dense Plasma layer

$$\beta_0 \equiv \frac{v_{osc}}{c} = \frac{e\mathcal{E}_0}{m_e \omega_0 c}$$

control parameter

Bifurcations to low-dimensional Chaos in B-SRS

see, Skoric et al. LIRPP1993; PRE1996

By varying the control (laser& plasma) parameters, Route to chaos in space-time in 3WI relativistic B-SRS is found : via steady-state, periodic, quasi-periodic and intermittent transition to chaos. Complexities in non-stationary bwd-Raman regimes include, strong spiky- burst like temporal Reflectivity & broadened blue-shifted incoherent spectra.

As the relative pump strength β_0 increases, starting from the value 0.01, the attractor changes according to the symbolic sequence

$$FP \rightarrow P \rightarrow QP \rightarrow I \rightarrow C$$

where FP stands for unimodal fixed point, P for periodic, QP for quasiperiodic, I for intermittent, and C for chaos. The quantitative boundaries in β_0 between successive attractors are depicted in Fig. 3.1.

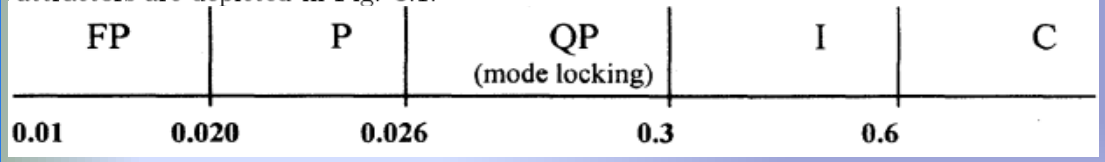

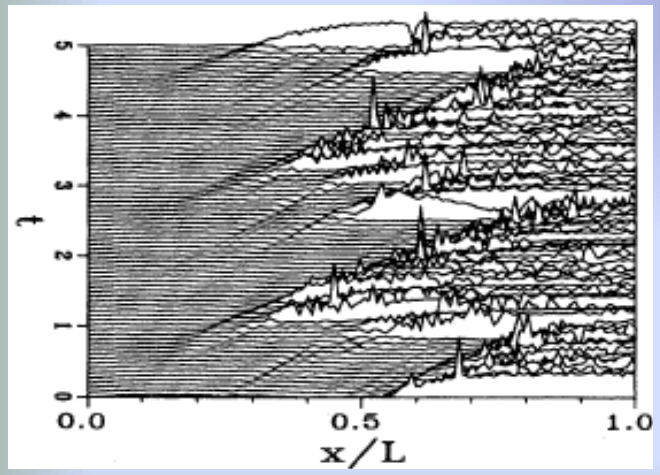

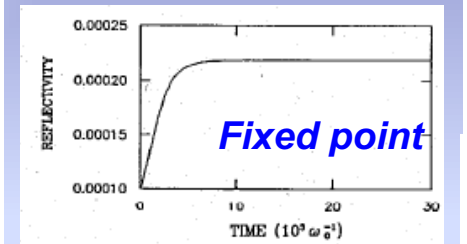

Figure 1:
Time evolution of the reflectivity of stimulated Raman backscattering for the parameters: $v_{osc} = 0.005\,c$, $\nu_e = 10^{-8}\,\omega_{pe}$, $n_0 = 0.1\,n_{cr}$, $L = 100\,c/\omega_0$, $T_e = 1\,\mathrm{keV}$.

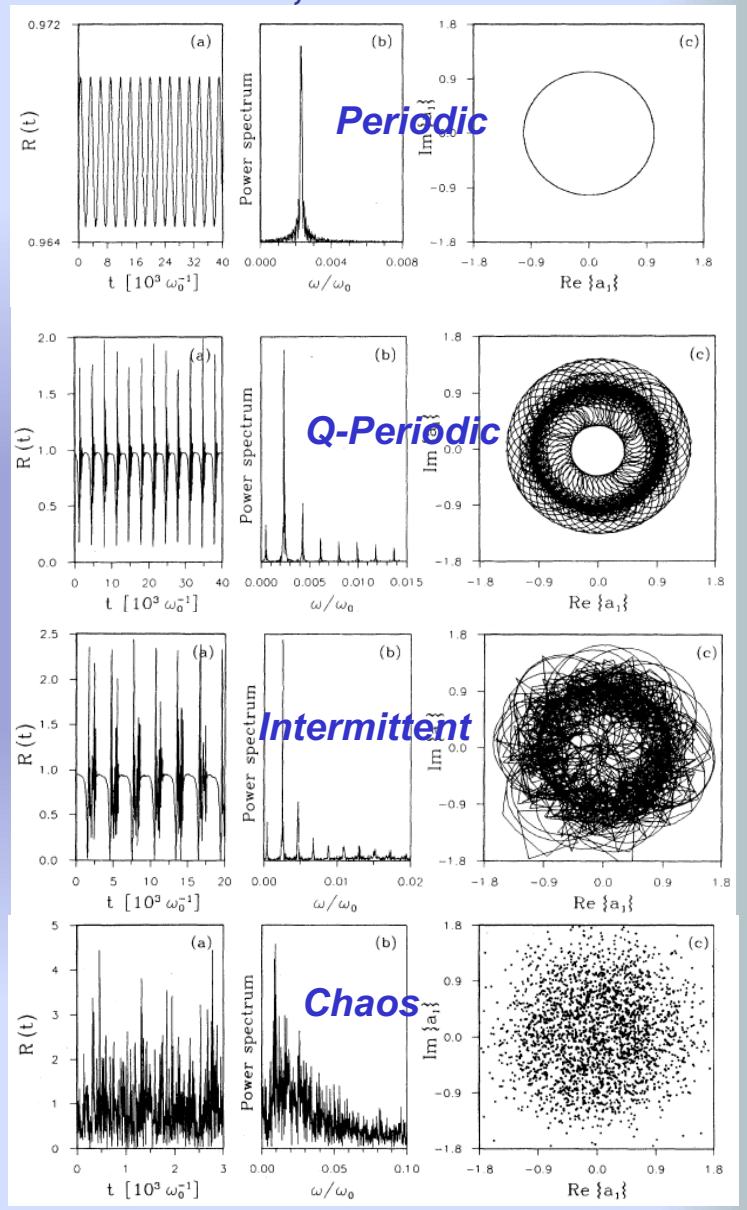

Reflectivity, power spectrum & phase diagram

EPW ST-Intermittency

Bifurcations to low-dimensional Chaos in B-SRS

By varying the control (laser& plasma) parameters, Route to chaos in space-time in 3WI relativistic B-SRS is found : via steady-state, periodic, quasi-periodic and intermittent transition to chaos. Complexities in non-stationary bwd-Raman regimes include, strong spiky- burst like temporal Reflectivity & broadened blue-shifted incoherent spectra.

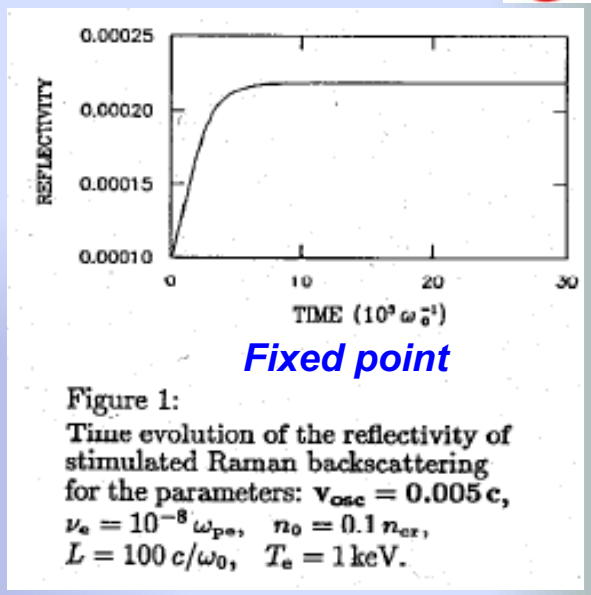

Fixed point

Figure 1:
Time evolution of the reflectivity of stimulated Raman backscattering for the parameters: $v_{osc} = 0.005\,c$, $\nu_e = 10^{-8}\,\omega_{pe}$, $n_0 = 0.1\,n_{cr}$, $L = 100\,c/\omega_0$, $T_e = 1\,\mathrm{keV}$.

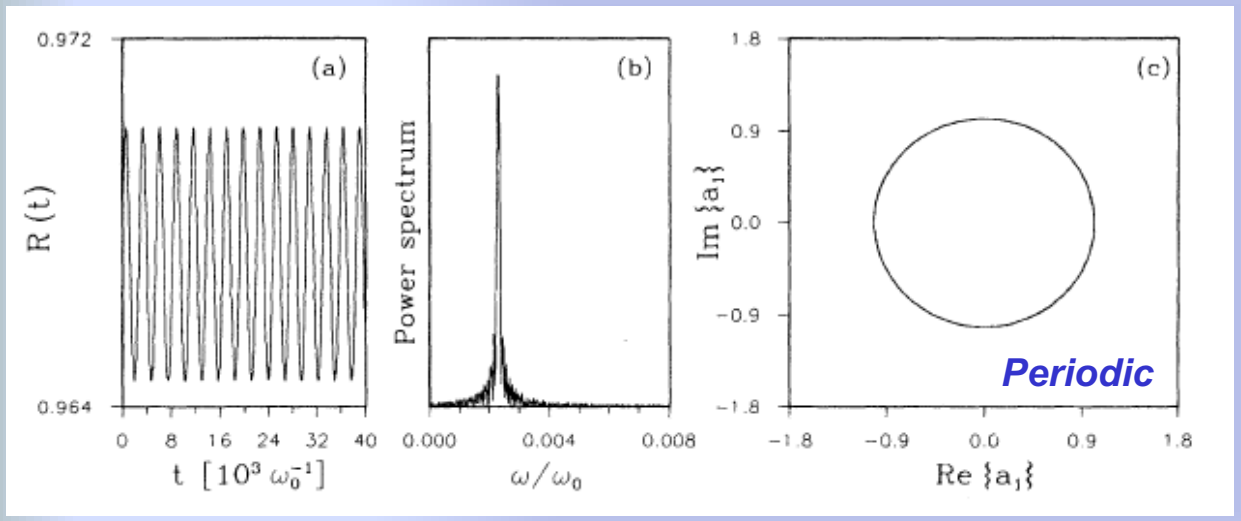

Periodic

Reflectivity, power spectrum & phase diagram

As the relative pump strength β_0 increases, starting from the value 0.01, the attractor changes according to the symbolic sequence

$$FP \rightarrow P \rightarrow QP \rightarrow I \rightarrow C$$

where FP stands for unimodal fixed point, P for periodic, QP for quasiperiodic, I for intermittent, and C for chaos. The quantitative boundaries in β_0 between successive attractors are depicted in Fig. 3.1.

see, Skoric et al. LIRPP1993; PRE1996

Bifurcations to low-dimensional Chaos in B-SRS

By varying the control (laser& plasma) parameters, Route to chaos in space-time in 3WI relativistic B-SRS is found : via steady-state, periodic, quasi-periodic and intermittent transition to chaos. Complexities in non-stationary bwd-Raman regimes include, strong spiky- burst like temporal Reflectivity & broadened blue-shifted incoherent spectra.

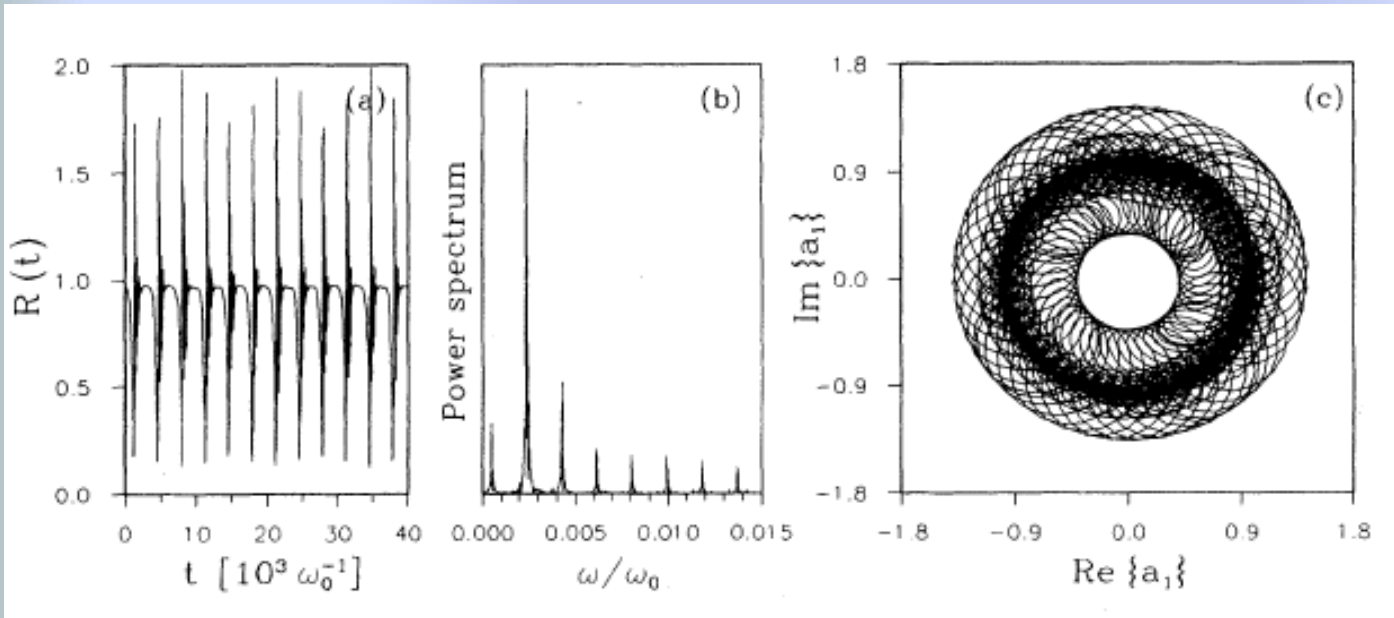

Quasi- Periodic

As the relative pump strength β_0 increases, starting from the value 0.01, the attractor changes according to the symbolic sequence

$$FP \to P \to QP \to I \to C$$

where FP stands for unimodal fixed point, P for periodic, QP for quasiperiodic, I for intermittent, and C for chaos. The quantitative boundaries in β_0 between successive attractors are depicted in Fig. 3.1.

see, Skoric et al. LIRPP1993; PRE1996

Bifurcations to low-dimensional Chaos in B-SRS

By varying the control (laser& plasma) parameters, Route to chaos in space-time in 3WI relativistic B-SRS is found : via steady-state, periodic, quasi-periodic and intermittent transition to chaos. Complexities in non-stationary bwd-Raman regimes include, strong spiky- burst like temporal Reflectivity & broadened blue-shifted incoherent spectra.

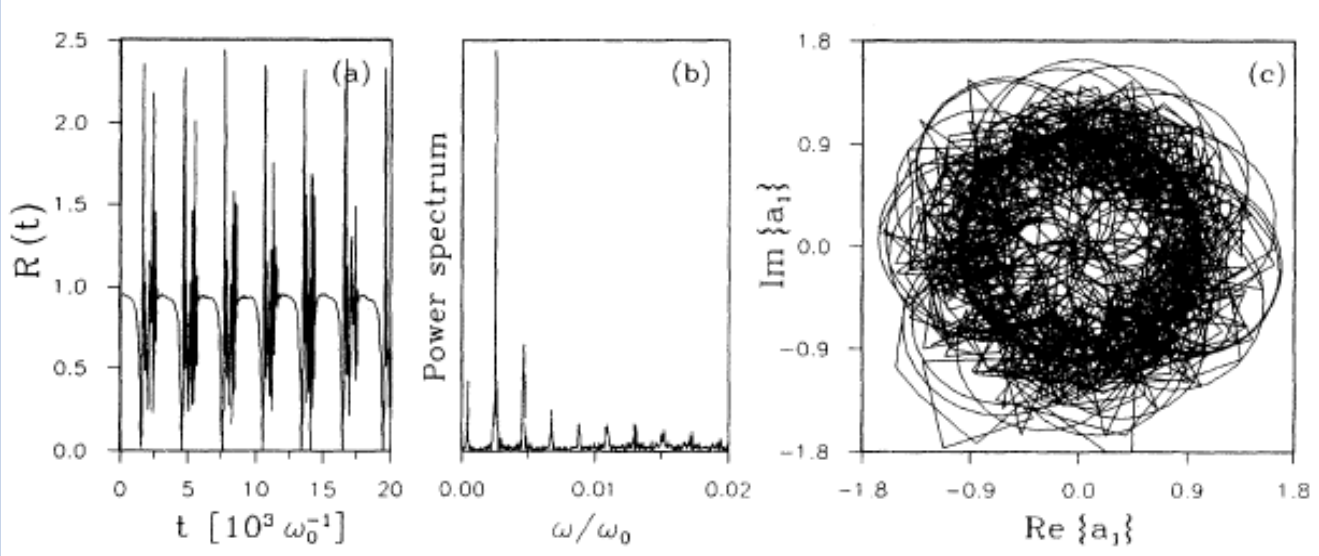

Reflectivity, power spectrum & phase diagram

Intermittency

As the relative pump strength β_0 increases, starting from the value 0.01, the attractor changes according to the symbolic sequence

$$FP \rightarrow P \rightarrow QP \rightarrow I \rightarrow C$$

where FP stands for unimodal fixed point, P for periodic, QP for quasiperiodic, I for intermittent, and C for chaos. The quantitative boundaries in β_0 between successive attractors are depicted in Fig. 3.1.

see, Skoric et al. LIRPP1993; PRE1996

Bifurcations to low-dimensional Chaos in B-SRS

By varying the control (laser& plasma) parameters, Route to chaos in space-time in 3WI relativistic B-SRS is found : via steady-state, periodic, quasi-periodic and intermittent transition to chaos. Complexities in non-stationary bwd-Raman regimes include, strong spiky- burst like temporal Reflectivity & broadened blue-shifted incoherent spectra.

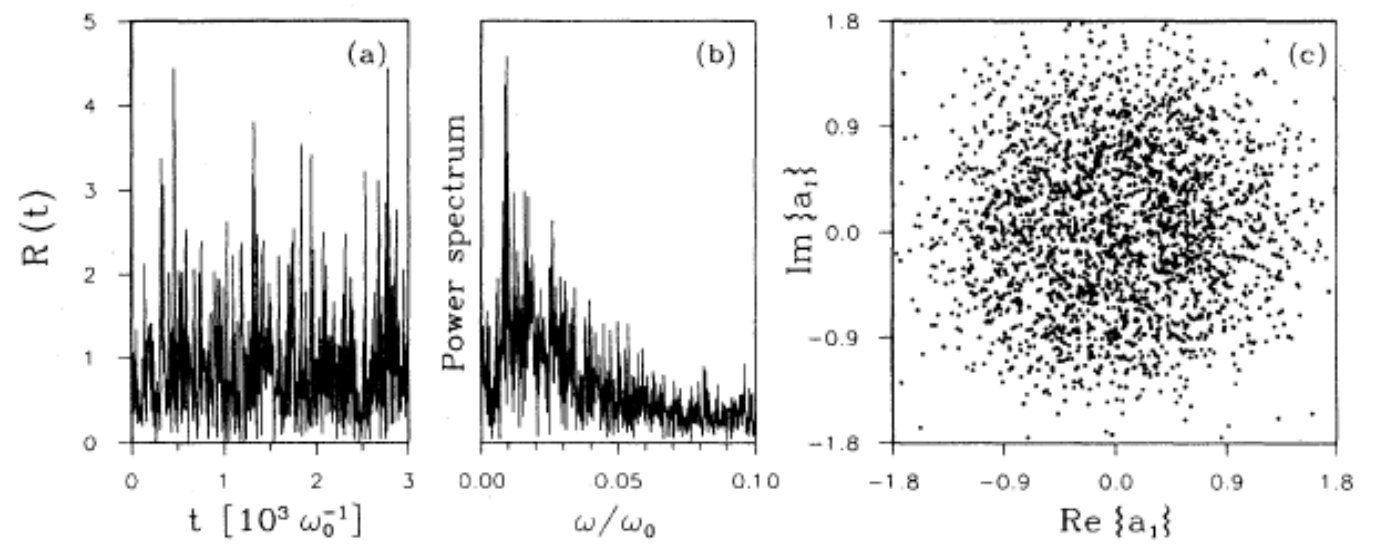

Chaos

Reflectivity, power spectrum & phase diagram

As the relative pump strength β_0 increases, starting from the value 0.01, the attractor changes according to the symbolic sequence

$$FP \rightarrow P \rightarrow QP \rightarrow I \rightarrow C$$

where FP stands for unimodal fixed point, P for periodic, QP for quasiperiodic, I for intermittent, and C for chaos. The quantitative boundaries in β_0 between successive attractors are depicted in Fig. 3.1.

see, Skoric et al. LIRPP1993; PRE1996

Bifurcations to low-dimensional Chaos in B-SRS

see, Skoric et al. LIRPP1993; PRE1996

By varying the control (laser& plasma) parameters, Route to chaos in space-time in 3WI relativistic B-SRS is found : via steady-state, periodic, quasi-periodic and intermittent transition to chaos. Complexities in non-stationary bwd-Raman regimes include, strong spiky- burst like temporal Reflectivity & broadened blue-shifted incoherent spectra.

As the relative pump strength β_0 increases, starting from the value 0.01, the attractor changes according to the symbolic sequence

$$FP \rightarrow P \rightarrow QP \rightarrow I \rightarrow C$$

where FP stands for unimodal fixed point, P for periodic, QP for quasiperiodic, I for intermittent, and C for chaos. The quantitative boundaries in β_0 between successive attractors are depicted in Fig. 3.1.

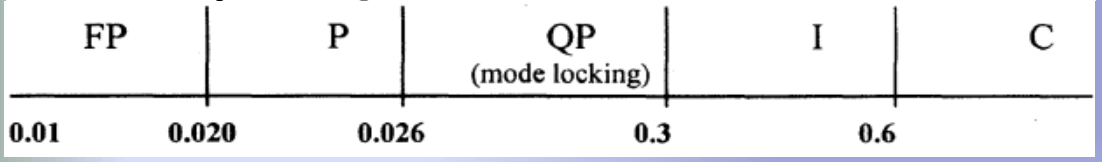

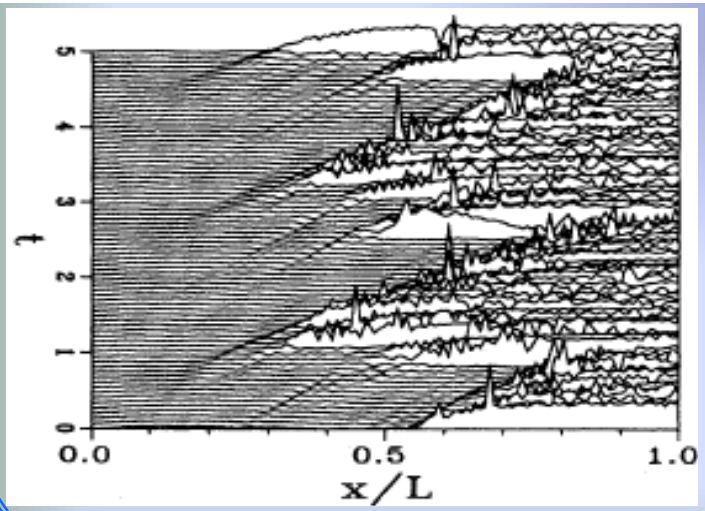

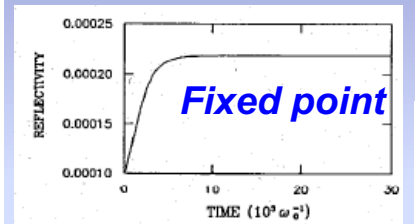

Figure 1:
Time evolution of the reflectivity of stimulated Raman backscattering for the parameters: $v_{osc} = 0.005\,c$, $\nu_e = 10^{-8}\,\omega_{pe}$, $n_0 = 0.1\,n_{cr}$, $L = 100\,c/\omega_0$, $T_e = 1\,\mathrm{keV}$.

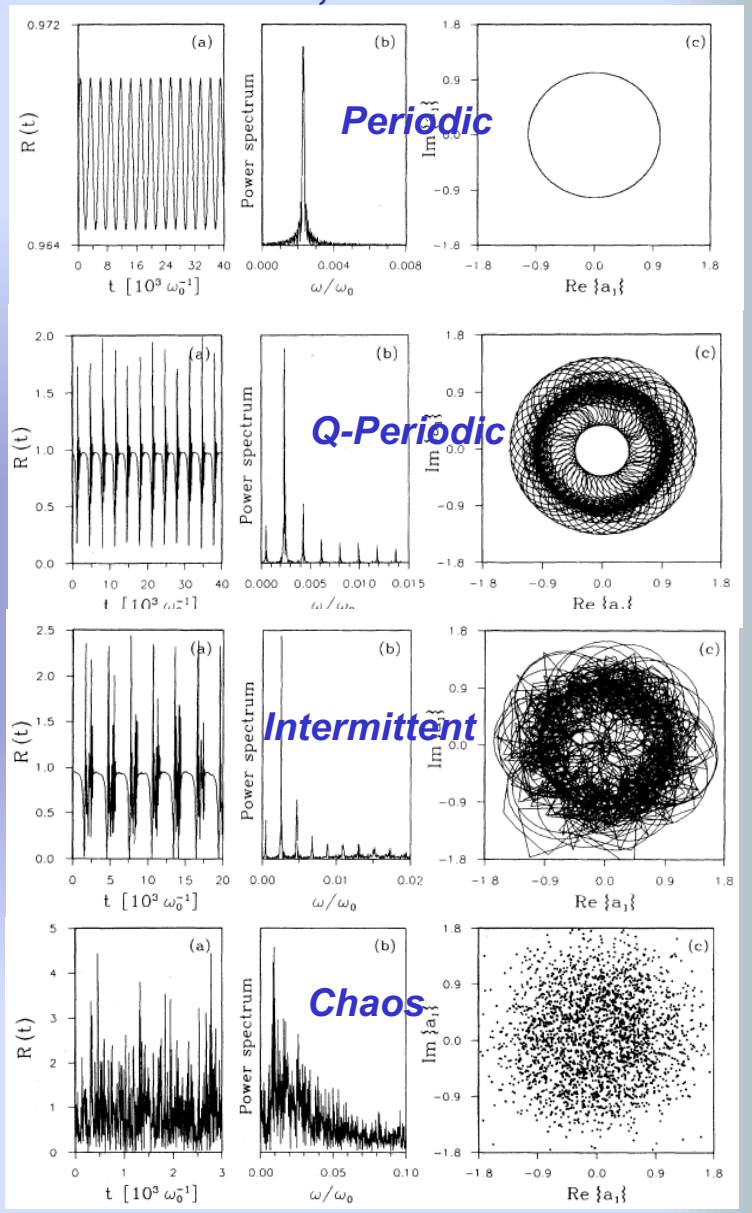

Reflectivity, power spectrum & phase diagram

EPW ST-Intermittency

Manly-Rowe breaks => Nonstationary relativistic SRS

Introducing the linear and nonlinear phase shift terms in the system of equations in the steady state ($\partial/\partial t \to 0$), conserved quantities (invariants) are calculated as $a_i(x,t) = A_i(x,t)\, e^{i\phi_i(x,t)}$ total phase shift is $\phi = \phi_0 - \phi_1 - \phi_2$

where A_i and ϕ_i, is the amplitude and phase of the wave ($i = 0, 1, 2$), respectively

$$\begin{aligned} m_0 &= V_0 n_0(x) - V_1 n_1(x) = const., \\ m_1 &= V_0 n_0(x) + V_2 n_2(x) = const., \\ K(x) &= A_0 A_1 A_2 \sin\phi - \frac{\sigma}{4} A_2^4 - \frac{\delta}{2} A_2^2 = const. \end{aligned} \tag{3.27}$$

Manly-Rowe relations

e.g. Forslund, PF 1975

with $n_i(x) = A_i(x)^2$, $i = 0, 1, 2$. For boundary conditions

$$n_0(0) = 1, n_1(L) = 0, n_2(0) = 0 \tag{3.28}$$

the third invariant becomes $K(0) = 0$. However, at the other boundary $x = L$, from (3.20), one calculates $K(L) \neq 0$; which breaks the invariance condition,i.e., $K(x) \neq const.$, hence, contradicts our basic assumption of the steady state. This simple argument, due to Škorić **(1997)** based on a nonlinear phase mismatch, explains a generic cause of nonstationarity in 3WI processes, such as, e.g. nonlinear stimulated Raman (also Brilloiun) instability saturation in laser plasma interactions

Manly-Rowe breaks => *Nonstationary* relativistic SRS

Introducing the linear and nonlinear phase shift terms in the system of equations in the steady state $(\partial/\partial t \to 0)$ conserved quantities (invariants) are calculated as

$a_i(x,t) = A_i(x,t)\, e^{i\phi_i(x,t)}$ total phase shift is $\phi = \phi_0 - \phi_1 - \phi_2$

where A_i and ϕ_i, is the amplitude and phase of the wave $(i = 0, 1, 2)$, respectively

$$
\begin{aligned}
m_0 &= V_0 n_0(x) - V_1 n_1(x) = const., \\
m_1 &= V_0 n_0(x) + V_2 n_2(x) = const., \\
K(x) &= A_0 A_1 A_2 \sin\phi - \frac{\sigma}{4} A_2^4 - \frac{\delta}{2} A_2^2 = const.
\end{aligned}
$$

Manly-Rowe relations

e.g. Forslund, PF 1975

with $n_i(x) = A_i(x)^2$, $i = 0, 1, 2$. For boundary conditions

$$n_0(0) = 1, n_1(L) = 0, n_2(0) = 0 \qquad (3.28)$$

the third invariant becomes $K(0) = 0$. However, at the other boundary $x = L$, from (3.20), one calculates $K(L) \neq 0$; which breaks the invariance condition,i.e., $K(x) \neq const$, hence, contradicts our basic assumption of the steady state. This simple argument, due to Škorić **(1997)** based on a nonlinear phase mismatch, explains a generic cause of nonstationarity in 3WI processes, such as, e.g. nonlinear stimulated Raman (also Brilloiun) instability saturation in laser plasma interactions

Generic cause for poor intensity scaling in B-SRS pulse amplification and incoherent spectral broadening, may be !?

e.g., Malkin & Fisch, PoP 2000-2006; see R. Trines, ICTP College 2007/2008

Intensity dependent spectral signatures in B-SRS

Intense temporal bursting, large incoherent broadening of blue shifted B-SRS spectra experimentally observed

see also, R.Trines, ICTP AIP 2007/08

In sub-ps relativistic laser-low-density plasma experiments, anomalous, intensity dependent, **modulated broadened blue shifted spectra**

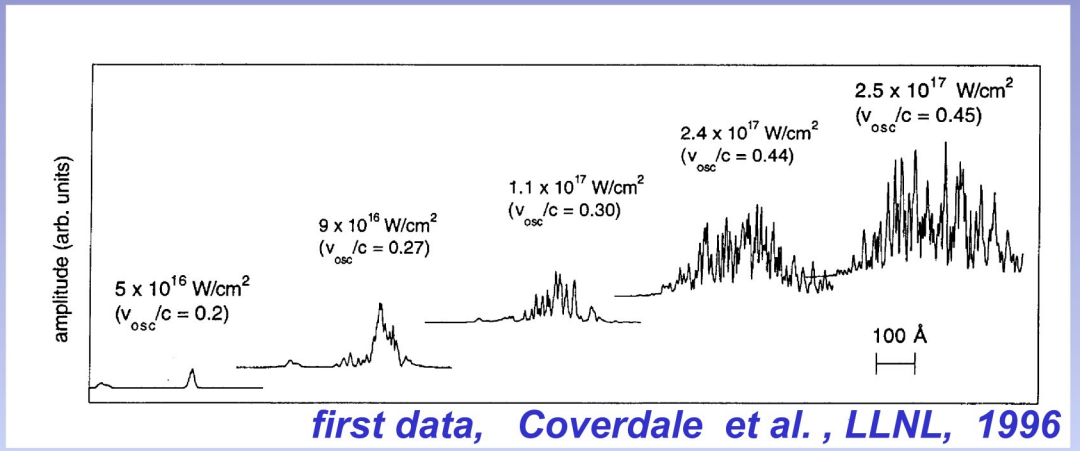

first data, Coverdale et al. , LLNL, 1996

Possible explanation is offered by the relativistic complexity in B-SRS !

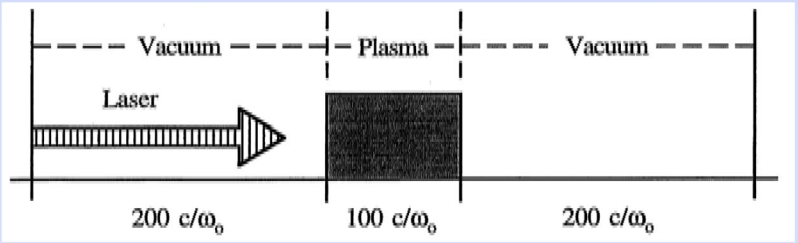

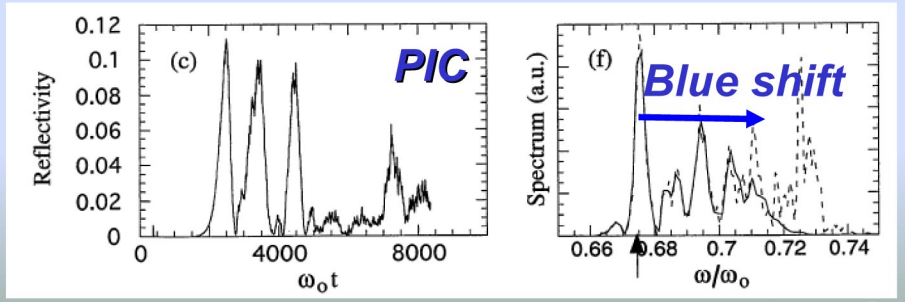

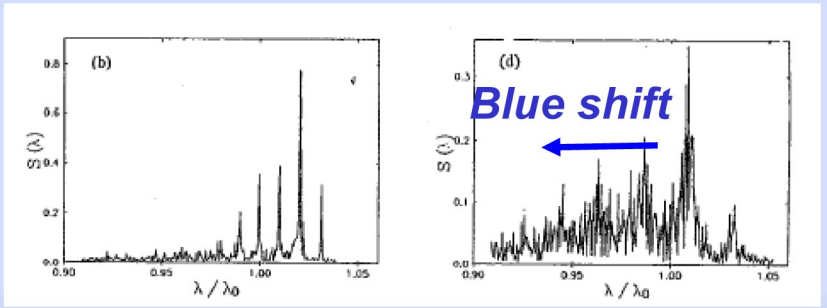

3WI model with rel. NLFS

Skoric, PRE1996; Miyamoto,JPSJ1998

FS pulse generation by B-SRS in a thin foil

Intensity scaling of proposed Raman pulse amplifications is limited !

e.g. by seeding short B-SRS pulse – but, schemes seems to work only at low intensities !?

e.g., Malkin & Fisch et al , PoP 2000-2006;
see review R. Trines, ICTP College 2007/2008

Root cause B-SRS transition to incoherence, maybe ?
predicted by simple 3WI model with relativistic NLFS
Skoric et al, 1993, 1996

Short QP pulsations in 3WI model with NLFS

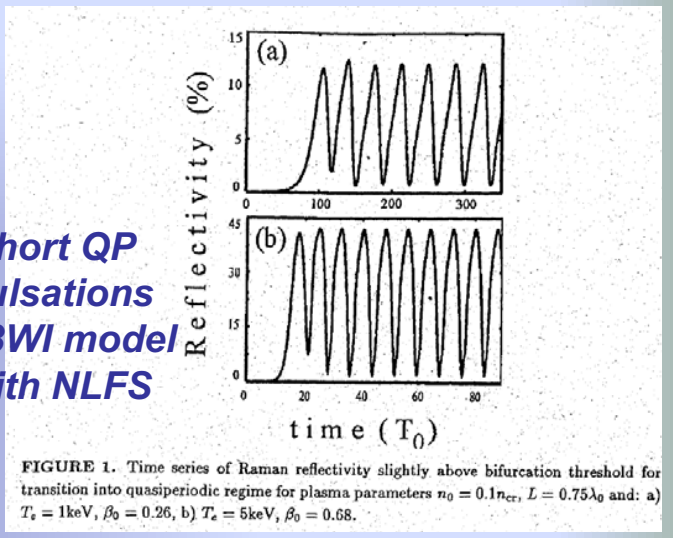

FIGURE 1. Time series of Raman reflectivity slightly above bifurcation threshold for transition into quasiperiodic regime for plasma parameters $n_0 = 0.1n_{cr}$, $L = 0.75\lambda_0$ and: a) $T_e = 1$keV, $\beta_0 = 0.26$, b) $T_e = 5$keV, $\beta_0 = 0.68$.

Alternative –B-SRS in very thin foil to exploit QP regime

PIC- kinetic dissipation isolates single Ultra-short FS pulse

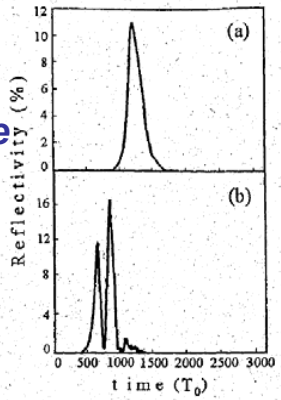

Miyamoto,1998

FIGURE 3. PIC simulation reflectivity versus time for two different pump intensities β_0: a) 0.02, b) 0.03. For the fundamental wavelength 1.06 μm, the pulse lengths are estimated to approximately 1 ps and 0.5 ps, respectively. Plasma is underdense: $n_0 = 0.1n_{cr}$, $T_e = 0.5$keV and $L = 16\lambda_0$.

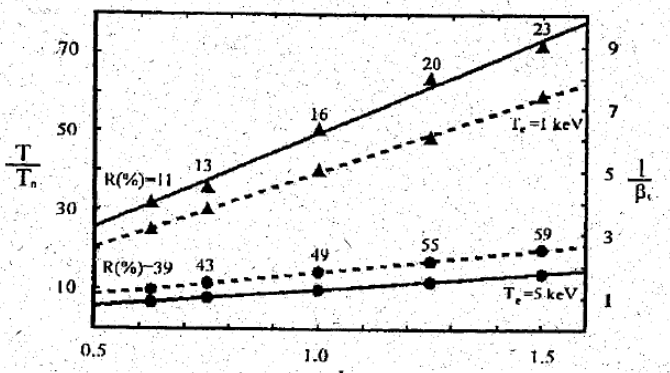

Scaling, down to ~ 20 FS

FIGURE 2. Pulse length T/T_0 (full line) and laser intensity β_0 (broken line) versus plasma foil thickness L with corresponding peak reflectivity for plasma temperatures of 1 keV (triangles) and 5 keV (dots). Plasma is underdense ($n_0 = 0.1n_{cr}$); λ_0 and T_0 are the laser wavelength and period, respectively.

Relativistic SRS & Stimulated Electron Acoustic Scattering

Recently, D. S. Montgomery PRL2001 reported observation of a novel Stimulated Electron Acoustic Wave backscattering (SEAS) to explain "single hot spot" experiments done at Trident laser facility

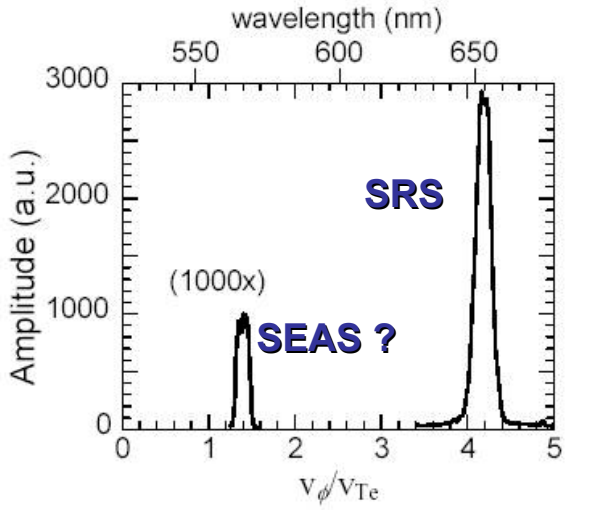

First observation of SEAS as reinterpretation of earlier data attributed to backward SRS

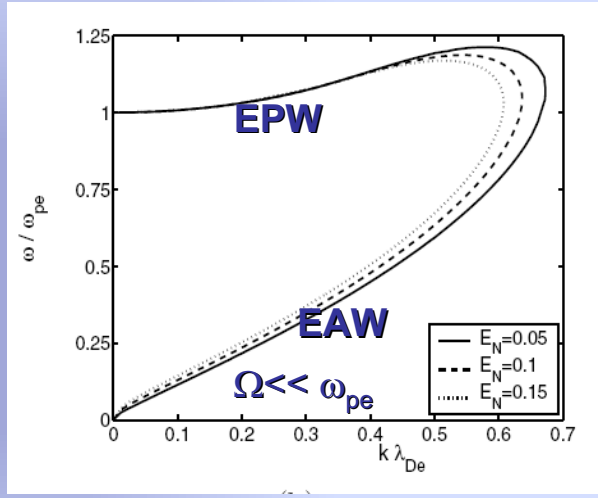

In linear theory, EAW is Landau damped in Vlasov-Maxwell system, since phase velocity is between EPW and IAW

Stix, 1962

However, *parametric instabilities* can excite strongly damped or plasma quasi-modes, and in particular, above is possible in relativistic plasmas with modified overlapping eigenmodes

Nishikawa & Liu, Adv. Pl. Phys. v.6 1976

Relativistic SRS and SEAS instabilities

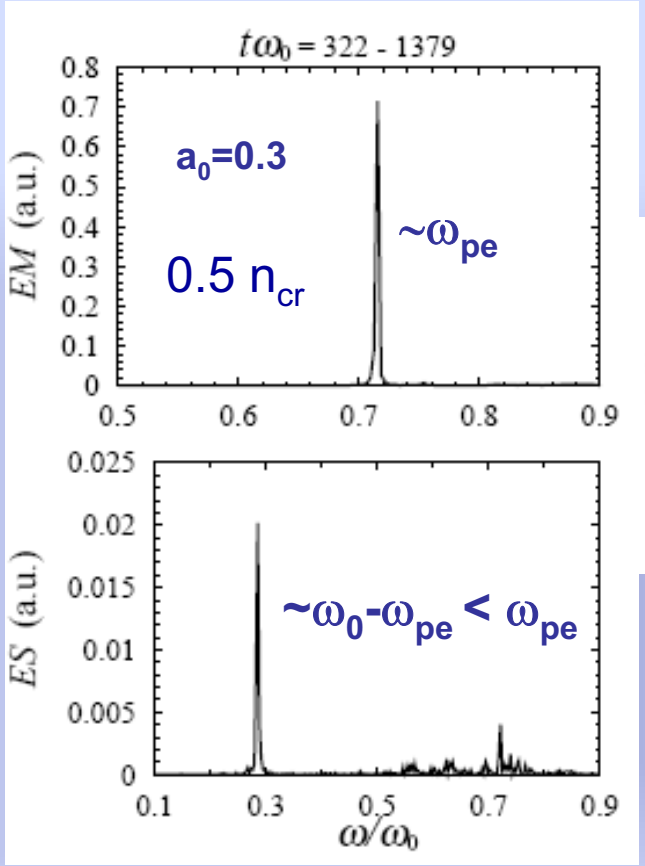

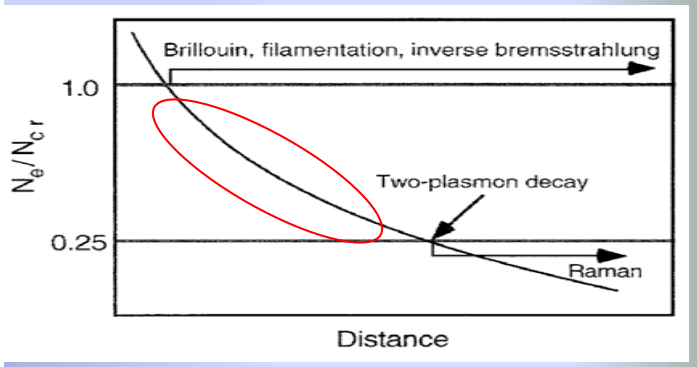

laser

subcritical

Nearly critical (ω~ω_{pe}) EM backscatter with V_s~ 0 => SEAS

Nikolic, Skoric, PRE2002

Relativistic SRS and SEAS instabilities

We propose a SEAS model as a resonant parametric coupling of three waves $a_i(x,t)\exp[i(k_i x - \omega_i t)]$, in a weakly varying envelope approximation [102, 105],

$$\frac{\partial a_0}{\partial t} + V_0 \frac{\partial a_0}{\partial x} = -M_0 a_s a_a, \tag{4.88}$$

$$\frac{\partial a_s}{\partial t} - V_s \frac{\partial a_s}{\partial x} = M_s a_0^* a_a, \tag{4.89}$$

$$\frac{\partial a_a}{\partial t} + V_a \frac{\partial a_a}{\partial x} + \Gamma_a a_a = M_a a_0^* a_s, \tag{4.90}$$

where $V_i > 0$ are the group velocities, Γ_a is damping rate for EAW ($\Gamma_0 = \Gamma_s = 0$ for light waves is used), $M_i > 0$ are the coupling coefficients and a_i are the wave amplitudes, where $i = 0, s, a$, stand for the pump, backscattered wave and EAW, respectively. Since considered model is a short plasma, in order to get high reflectivity, instability needs to be absolute. With standard boundary conditions $a_0(0,t) = E_0$, $a_s(L,t) = a_a(0,t) = 0$, the backscattering becomes an absolute instability if

$$L/L_0 > \pi/2, \tag{4.91}$$

[91, 105], where $L_0 = (V_s V_a)^{1/2}/\gamma_0$ is the interaction length and $\gamma_0 = E_0(M_s M_a)^{1/2}$ is the uniform growth rate. Since observed $V_s \approx 0$ for the backscatter, the condition (4.91) is readily satisfied ($L_0 \approx 0$). Explicit form of (4.88) and (4.89) is easy to get (light waves),

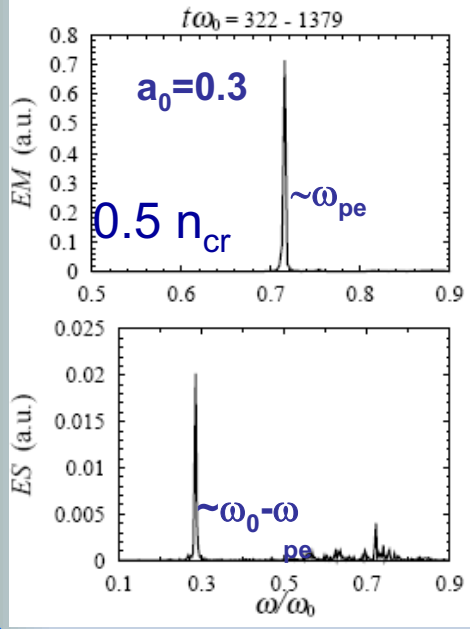

Nearly critical ($\omega \sim \omega_{pe}$) EM backscatter with $V_s \sim 0$ => SEAS

Nikolic, Skoric, PRE2002

SRS and SEAS Instabilities

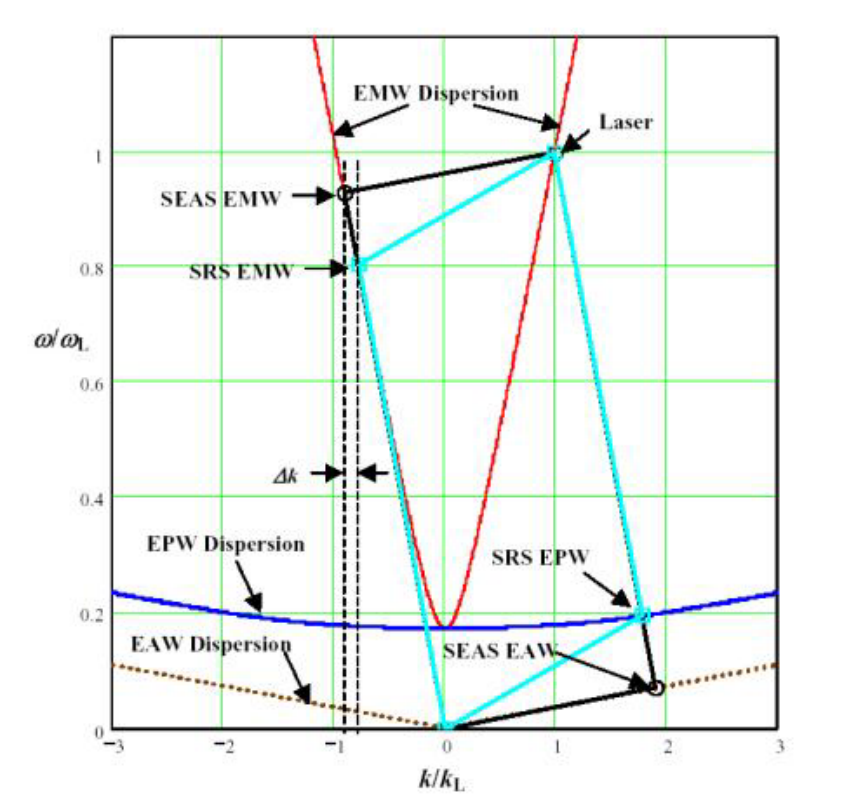

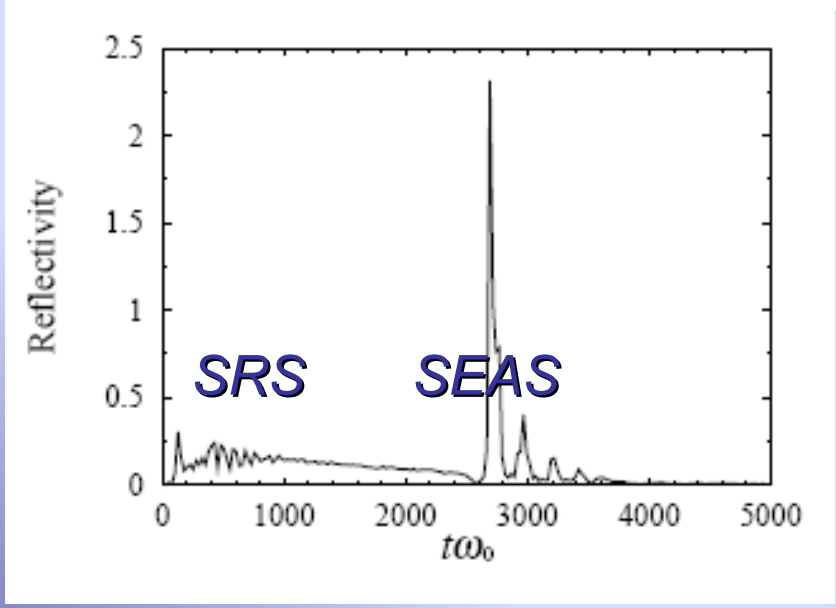

Reflectivity in time from two connected plasma ($L_{1,2}$) layers with densities sub- and over-critical for SRS. Initial bursts by relativistic SRS follows at late times *Intense SEAS pulse* in L_2, heated by SRS electrons

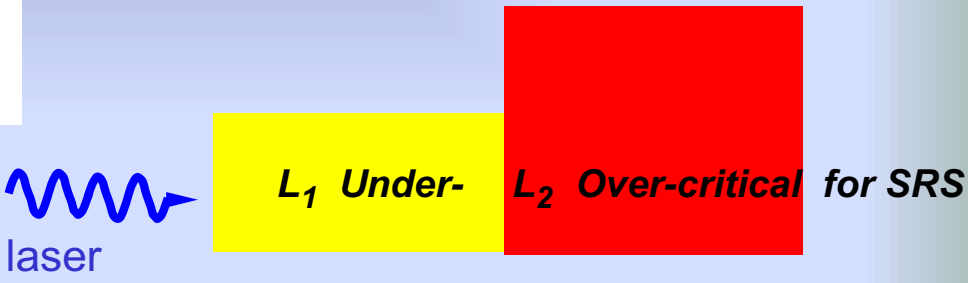

SRS Cascade into Photon Condensation

A nonlinear interplay between backward and forward SRS, produces a strong spatial modulation of the laser light pulse and the down cascade in frequency spectrum. *Raman Cascade* saturates by a unique *Photon Condensation* at the bottom of the light spectrum near the electron plasma frequency, related to strong depletion and often break-up of the laser beam. In the final stage of the cascade-into-condensate mechanism, depleted downshifted laser pulse gradually transforms into a train of ultra-short relativistic light solitons. The interaction of a relativistic laser pulse with an *underdense* plasma is studied by fluid-Maxwell and particle-in-cell simulation

see, Skoric, Mima et al., APS2000; PoP 2001

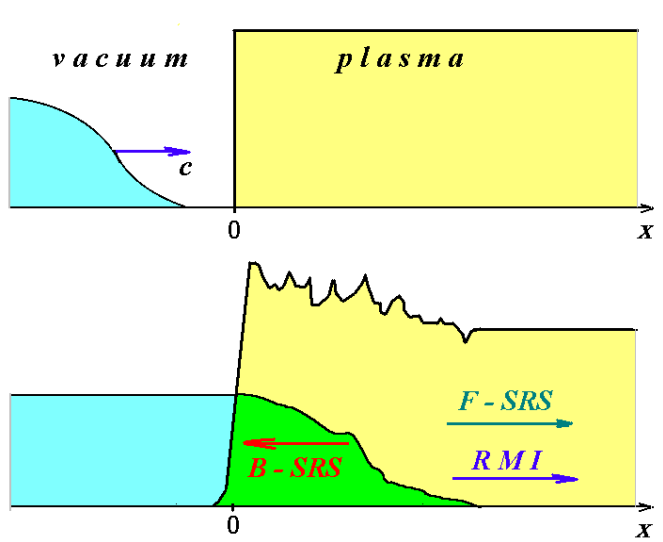

$$\omega_0 \geq 2\omega_{pe} \implies n \leq \gamma n_{cr}/4$$

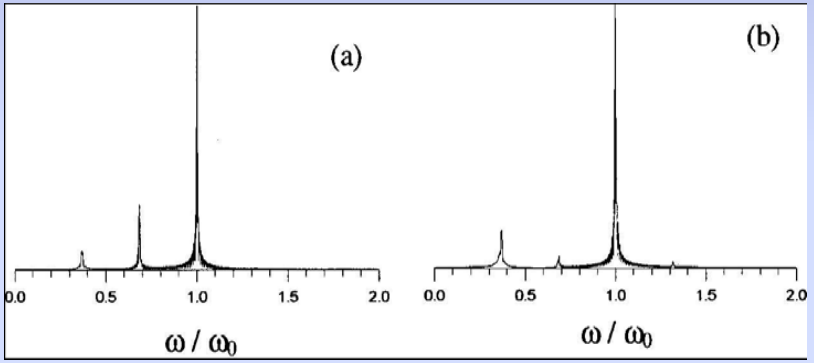

F-SRS Cascade-into-condensate (n~0.1 n_c; a_0=0.1)

$$\omega_{s,j} = \omega_0 \pm j\omega_{epw} \quad ; \quad \pm k_{s,j} = k_0 \pm jk_{epw}$$

Higher order Stokes and anti-Stokes hamonics and interplay between Fwd and Bwd- SRS

Relativistic 1D fluid-Maxwell simulations

Long linearly polarized laser pulse enters underdense plasma in *x*-direction, inducing both transverse and longitudinal electron motion. In 1D case, longitudinal (E_x) and transverse (E_y) electric Field and magnetic field B_z

$$\frac{\partial E_x}{\partial t} = \frac{n_e p_x}{\gamma},$$

$$\frac{\partial E_y}{\partial t} + \frac{\partial B_z}{\partial x} = \frac{n_e A}{\gamma},$$

$$\frac{\partial B_z}{\partial t} + \frac{\partial E_y}{\partial x} = 0,$$

$$\frac{\partial A}{\partial t} = -E_y,$$

Maxwell eqs, in 1D Coulomb gauge

$$\gamma = \left(1 + p_x^2 + A^2\right)^{1/2}$$

$$\frac{\partial n_e}{\partial t} = -\frac{\partial}{\partial x}\left(\frac{n_e p_x}{\gamma}\right),$$

$$\frac{\partial p_x}{\partial t} = -E_x - \frac{\partial \gamma}{\partial x},$$

Continuity and electron eq. of motion

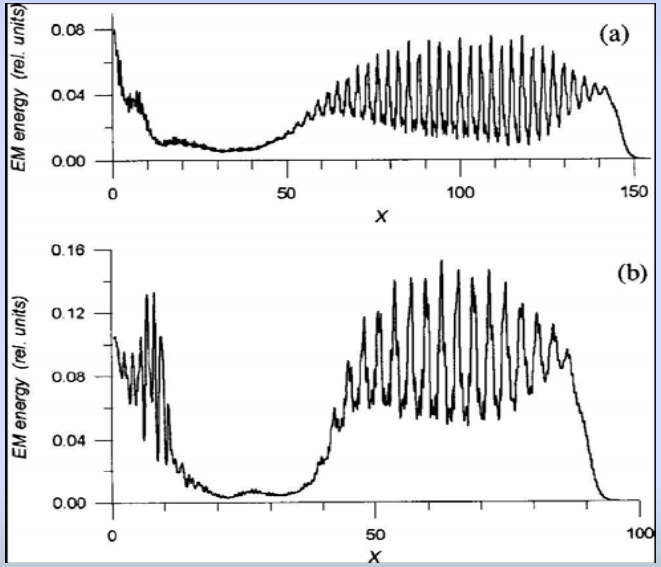

Snapshots of EM energy in space

Stimulated Raman Cascade-into-Condensate

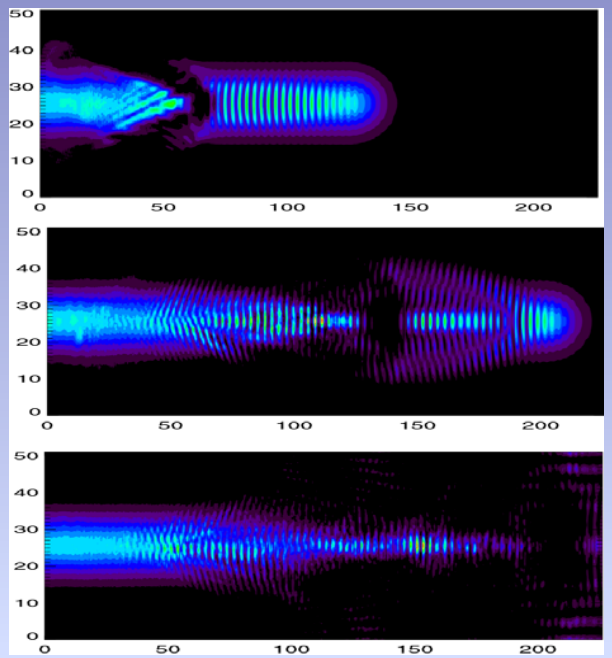

Beam break-up

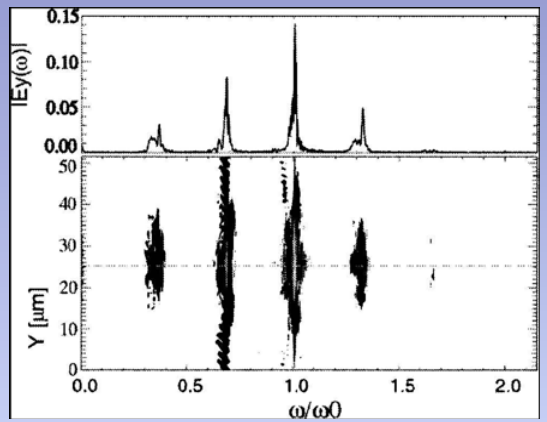

Intensity & F-SRS spectrum by 2D PIC

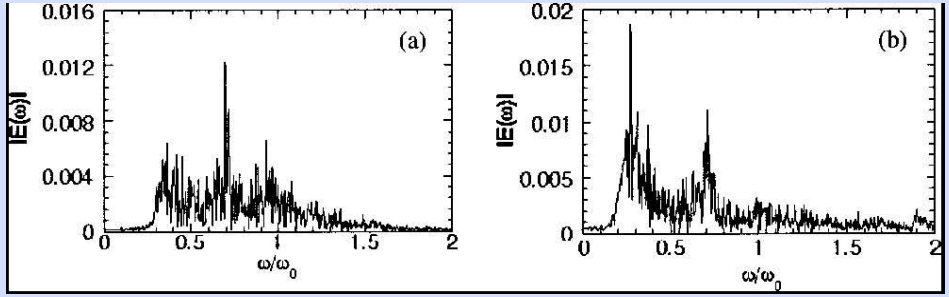

B-SRS spectrum (n~0.05 n_c)- 1D PIC

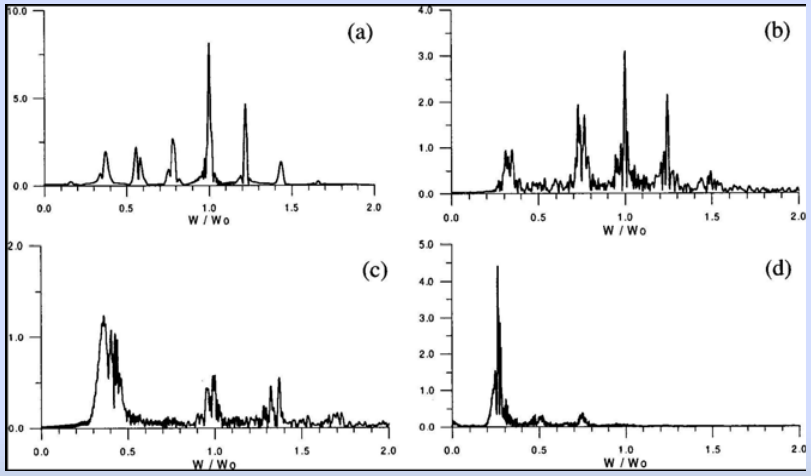

F-SRS spectrum (n~0.05 n_c)- 1D PIC

Self-organization in relativistic laser-underdense plasmas

Stimulated Photon Cascade into Condensation

Nonlinear interplay between backward and forward SRS produces strong spatial modulation of relativistic light pulse and down cascade in frequency spectrum. Raman *Cascade* saturates by a unique *Photon Condensation* at the bottom of the light spectrum bellow the electron plasma frequency with strong depletion and break-up of laser beam. Finally, pulse is transformed into a train of ultra-relativistic spatially localized EM structures- *Solitons*

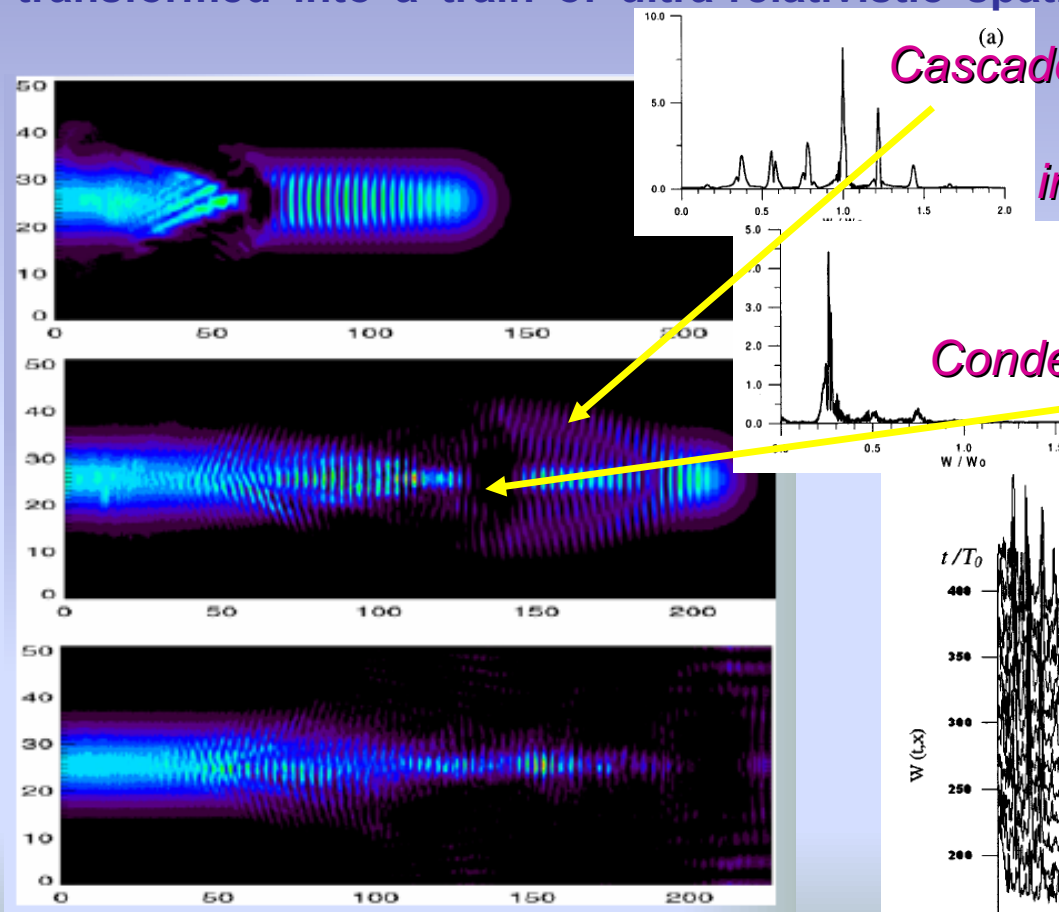

Mima, Jovanovic, Sentoku, Z-M Sheng & Skoric, APS-2000, PoP 2001

2D PIC simulations (snapshots)

Relativistic EM Solitons in plasmas

Relativistic EM Solitons: Stationary spatially localized EM structures, self-trapped in a local change of plasma index of refraction due to: relativistic electron mass decrease and density drop caused by ponderomotive force of laser pulse

Stationary, localized solutions of nonlinear partial differential equations (PDF)

$$\Delta\vec{A} - \frac{1}{c^2}\frac{\partial^2\vec{A}}{\partial t^2} = -\mu_0\vec{J}_\perp$$

$$\Delta\Phi = -\frac{\rho}{\varepsilon_0}$$

$$\frac{d}{dt}(\vec{p} - e\vec{A}) = -e[\nabla\Phi - (\nabla\vec{A})\cdot\vec{v}]$$

Circular polarization

$$A(x,t) = \frac{2\lambda\cosh(\lambda x)}{\cosh^2(\lambda x) - \lambda^2}\exp(i\sqrt{1-\lambda^2}\,t, \quad \omega = \sqrt{1-\lambda^2}$$

Solitons ! - Stable nonlinear localized waveforms

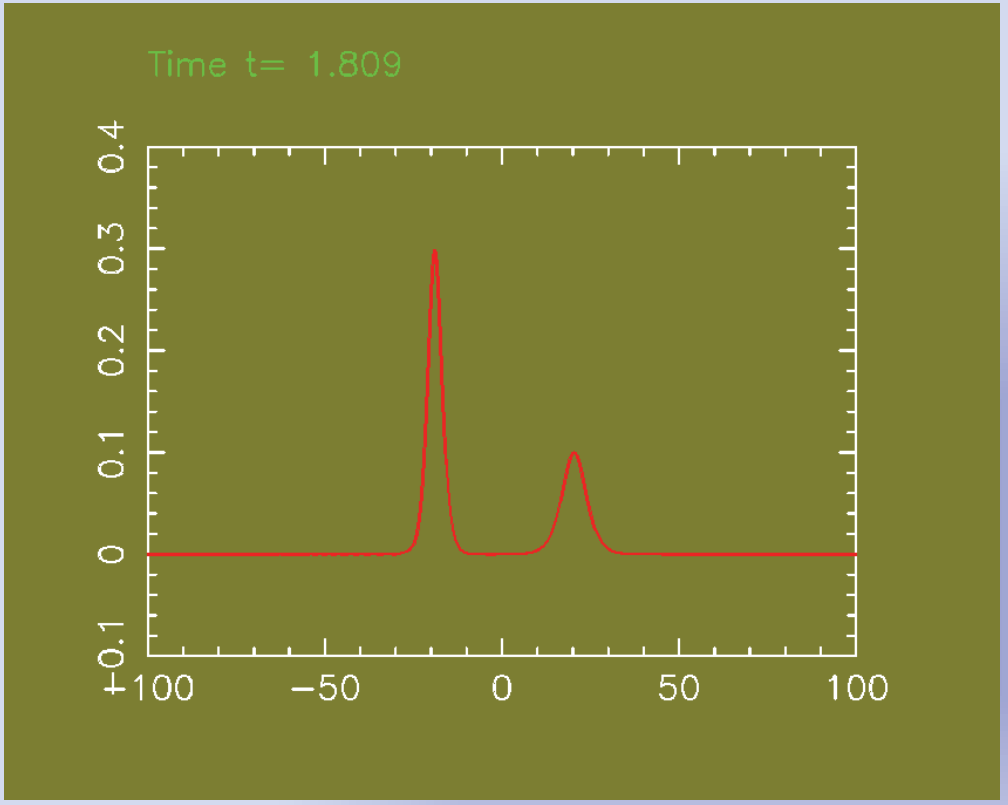

Solitons in many physical problems –very remarkable properties - elastic collisions

$$u_t + 6\,u\,u_x + u_{xxx} = 0$$

$$u(x,t) = \frac{1}{2}\,\mathrm{sech}^2\frac{1}{2}\sqrt{c}\,(x - ct + \delta)\,,$$

KdV soliton

Solitons – solutions of nonlinear PDEs, e.g., Korteweg-de-Vries, Sine-Gordon eq. Nonlinear Schroedinger equation, etc.

Discovery of the Soliton by Scott Russell in 1834

Large stable Solitary wave- soliton observed in water Canal

Soliton on the Scott Russell Aqueduct on the Union Canal in Edinburgh, Scotland, 1995

Fluid -Maxwell equations

Nonlinear relativistic 1D equation for cold plasma

$$\left(\frac{\partial^2}{\partial t^2} - c^2\frac{\partial^2}{\partial x^2}\right)a = -\frac{\omega_p^2}{n_0}\frac{n}{\gamma}a$$

$$\frac{\partial n}{\partial t} + \frac{\partial}{\partial x}\left(\frac{np}{m\gamma}\right) = 0$$

$$\frac{\partial p}{\partial t} = -eE_{\parallel} - mc^2\frac{\partial \gamma}{\partial x}$$

$$\gamma = (1 + a^2 + p^2/m^2c^2)^{1/2}$$

$a = eA/mc^2$ - Vector potential (y-axis)

$\omega_p = (4\pi e^2 n_0/m)^{1/2}$ electron plasma frequency

$E_{\parallel}$ - Longitudinal electric field

p - electron momentum (x-direction)

n - electron density

n_0 - zero order electron density

Laser Pulse ***Linear Polar.***

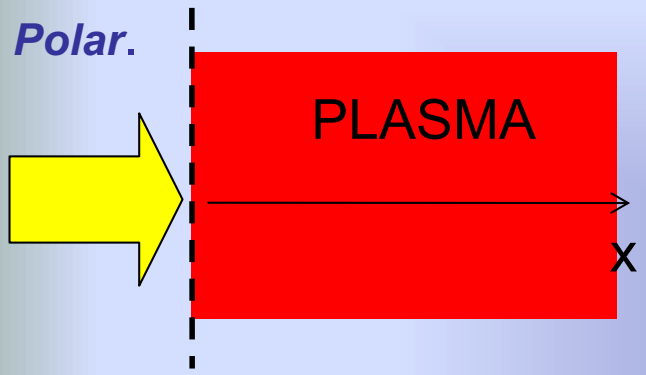

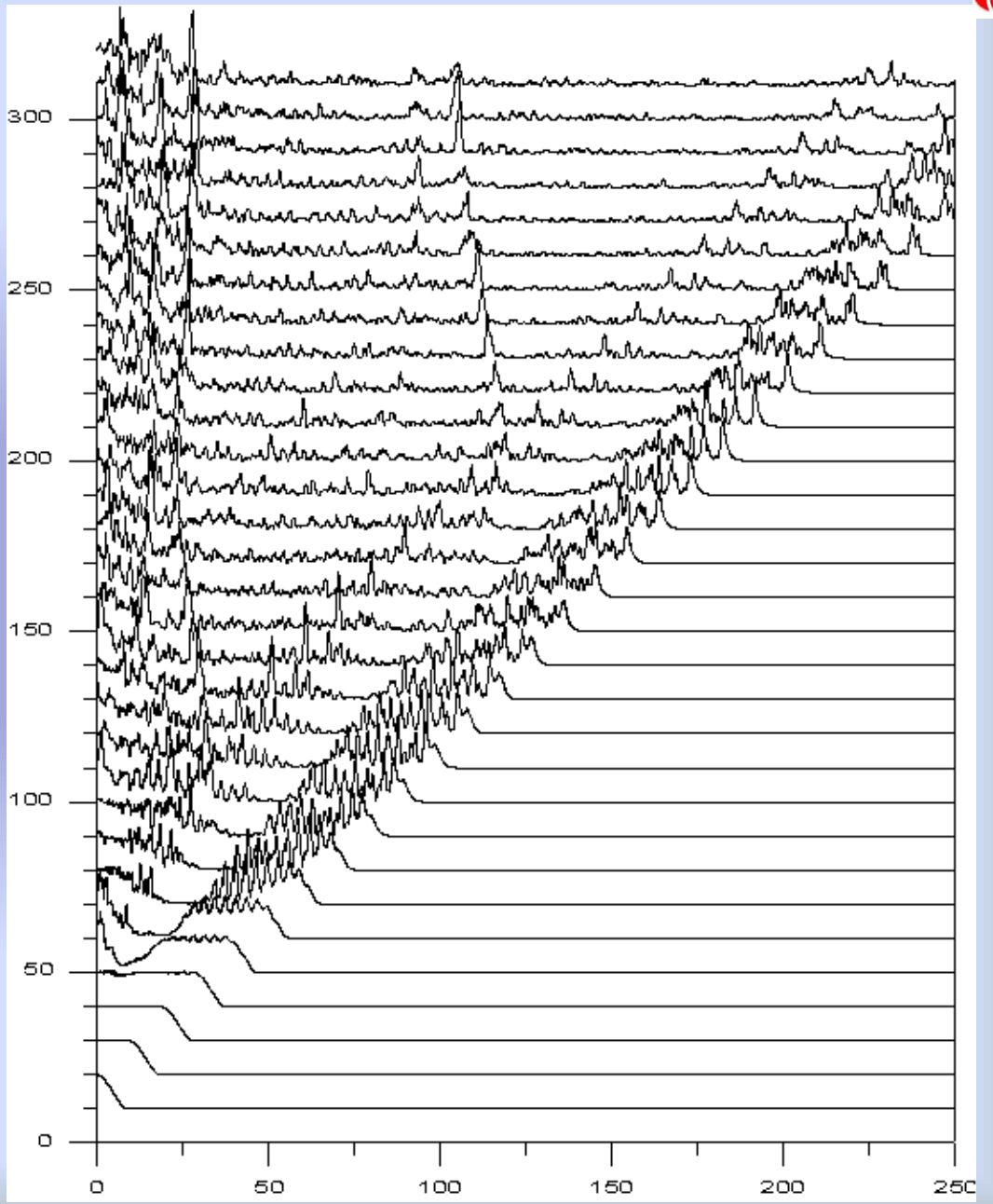

Space-Time evolution of EM energy density

1D fluid-Maxwell simulation of laser pulse a_0=0.5 and ω_0=3.2 ω_p

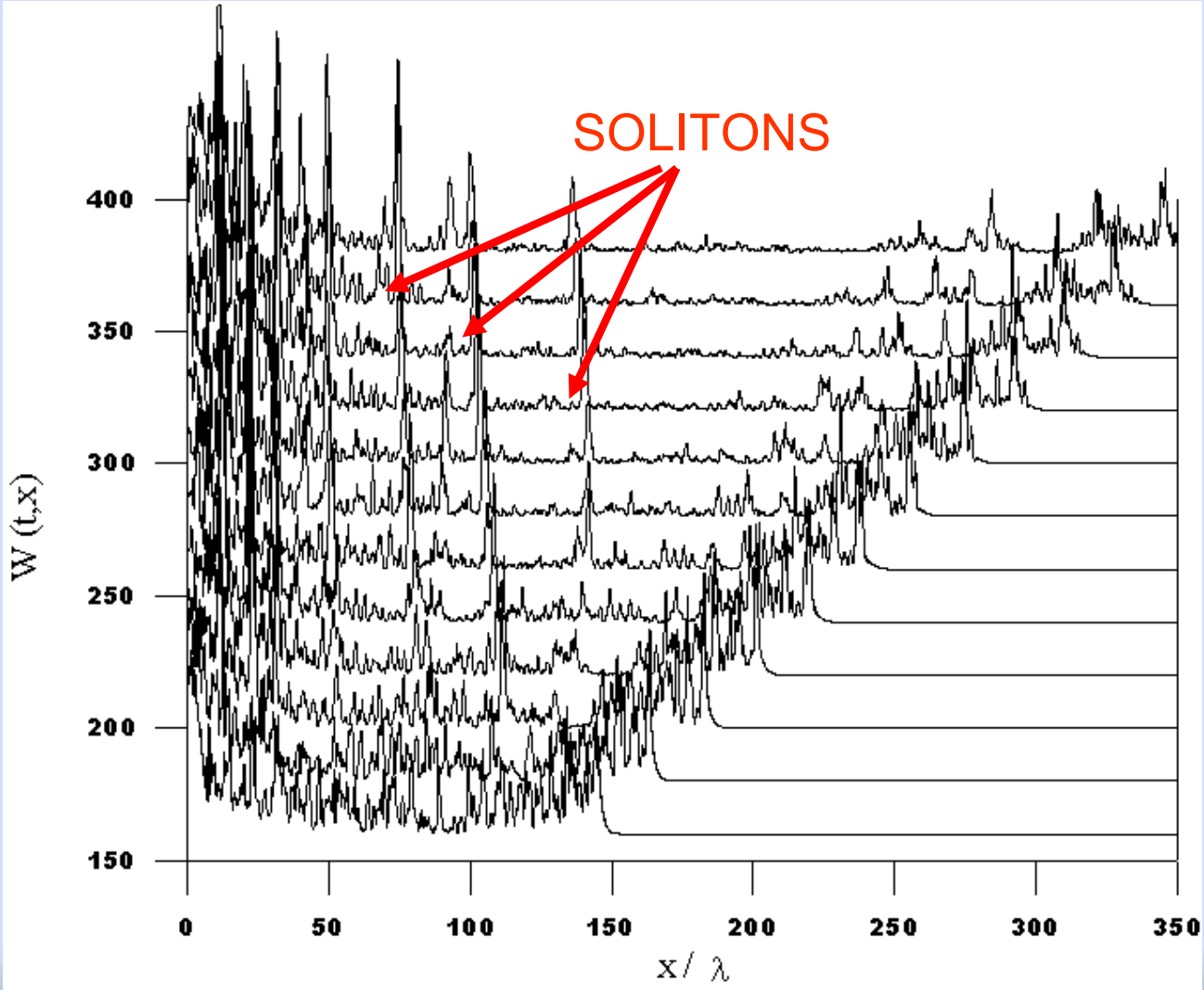

Weakly - relativistic 1D equation

Dimensionless units:

$$\delta n = (n - n_0)/n_0$$

$$x \to (c\omega_p^{-1})x$$

$$t \to (\omega_p^{-1})t$$

Conditions:

$$|a| << 1$$

$$|\delta n| << 1$$

$$\left(\frac{\partial^2}{\partial t^2} - \frac{\partial^2}{\partial x^2}\right)a = -\left(1 + \delta n - \frac{a^2}{2}\right)a$$

$$\frac{\partial^2 \delta n}{\partial t^2} + n = \frac{1}{2}\frac{\partial^2}{\partial x^2}a^2$$

Linear polarization
Slowly-varying complex amplitudes

$$a = \frac{1}{2}\left[A e^{-it} + A^* e^{it}\right]$$

Only odd harmonics

$$\delta n = N_0 + \frac{1}{2}\left(N_2 e^{-i2t} + N_2^* e^{i2t}.\right)$$

Only even harmonics

GENERALIZED NONLINEAR SCHRÖDINGER (GNLS) EQUATION

$$i\frac{\partial A}{\partial t} + \frac{1}{2}A_{xx} + \frac{3}{16}|A|^2 A - \frac{1}{8}(|A|^2)_{xx} A + \frac{1}{24}(A^2)_{xx} A^* = 0$$

$$N_0 = \frac{1}{4}(|A|^2)_{xx}$$

$$N_2 = -\frac{1}{6}(A^2)_{xx}$$

CONSERVED QUANTITIES

Photon number

$$P = \int |A|^2 \, dx,$$

Hamiltonian

$$H = \frac{1}{2}\int \left\{ |A_{xx}|^2 - \frac{3}{16}|A|^4 - \frac{1}{8}[(|A|^2)_x]^2 - \frac{1}{6}|A|^2 |A_x|^2 \right\} dx$$

SOLITON SOLUTION $A = \alpha(x) e^{i\lambda^2 t}$

$$\pm \lambda x = \frac{1}{2\sqrt{2}} \ln \frac{\sqrt{1 - \frac{3}{32}\frac{\alpha^2}{\lambda^2}} + \sqrt{1 - \frac{\alpha^2}{3}}}{\left| \sqrt{1 - \frac{3}{32}\frac{\alpha^2}{\lambda^2}} - \sqrt{1 - \frac{\alpha^2}{3}} \right|} - \frac{4}{3}\lambda \ln \frac{\frac{1}{3}\sqrt{32\lambda^2 - 3\alpha^2} + \sqrt{1 - \frac{\alpha^2}{3}}}{\sqrt{\left| 1 - \frac{32}{9}\lambda^2 \right|}}$$

amplitude

$$\alpha_0 = \frac{4\sqrt{2}}{\sqrt{3}}\lambda$$

"cusp" soliton

$$\lambda \geq \lambda_c = 3/4\sqrt{2} \quad (\alpha_0 \geq \sqrt{3})$$

NLS soliton

$$\lambda << \lambda_c$$

SOLITON SOLUTION (CIRCULAR POLARIZATION)

$$a(x,t) = \frac{2\lambda \cosh(\lambda x)}{\cosh^2(\lambda x) - \lambda^2} \exp(i\sqrt{1-\lambda^2}\, t)$$

amplitude

$$a_0 = \frac{2\lambda}{1-\lambda^2}$$

frequency of polarization plane

$$\omega = \sqrt{1-\lambda^2}$$

limitations

$$a_o < \sqrt{3}$$

$$1 > \omega > \sqrt{2/3} \qquad \left(0 < \lambda < \sqrt{3}/3\right)$$

SOLITON STABILITY

Criteria for soliton stability (Vakhitov-Kholokolov)

$$\frac{dP_o}{d\lambda^2} > 0,$$

Linear polarization

$$P_o(\lambda) = \frac{16}{3}\lambda + \frac{2}{\sqrt{2}}\left(1 - \frac{32}{9}\lambda^2\right)\ln\frac{1+\frac{4\sqrt{2}}{3}}{\left|1-\frac{4\sqrt{2}}{3}\right|}$$

Circular polarization

$$P_o(\lambda) = \frac{4\arctan\left(\frac{\lambda}{\sqrt{1-\lambda^2}}\right)}{(1-\lambda^2)^{3/2}} + \frac{4\lambda}{1-\lambda^2}$$

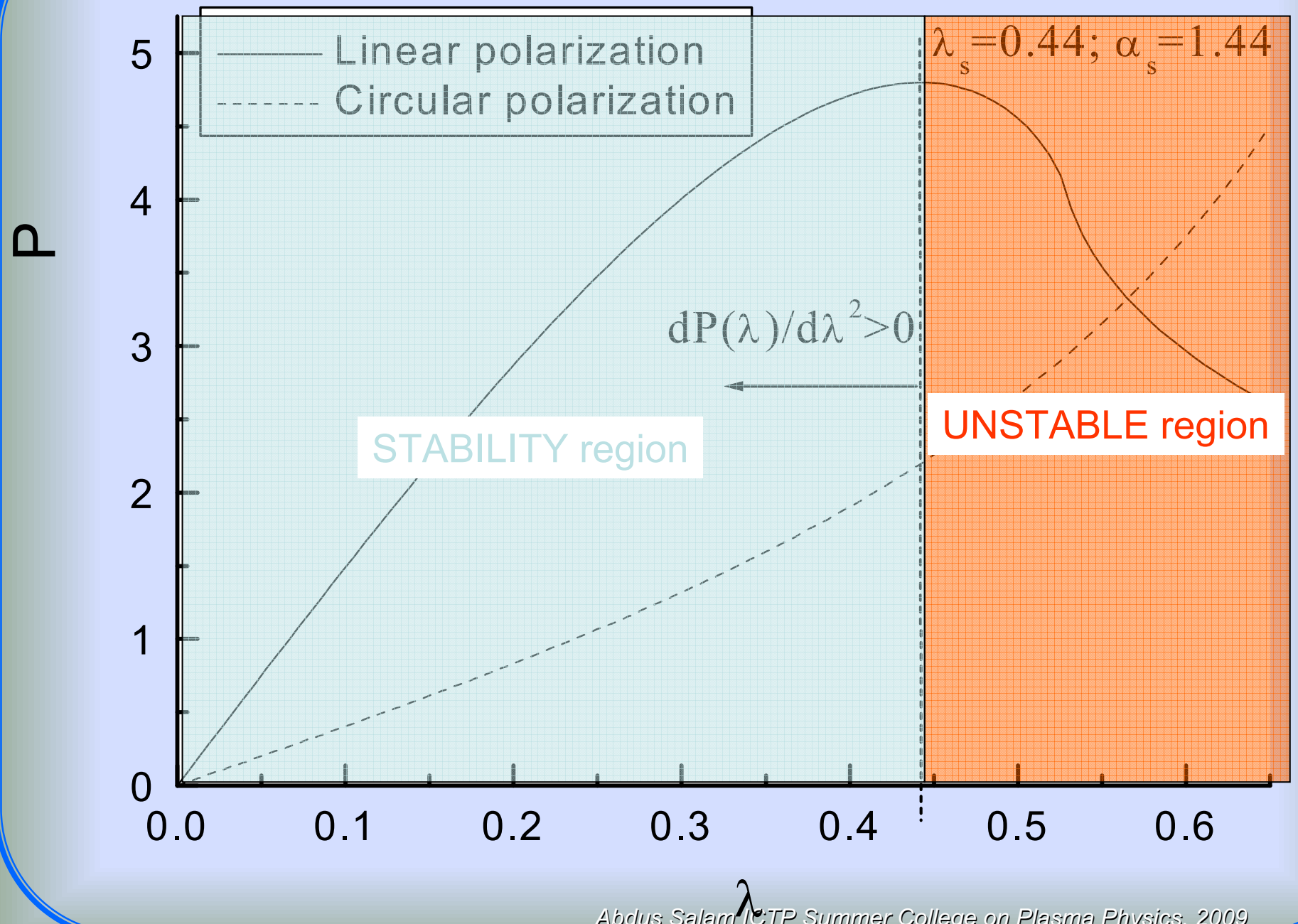
Linear polarization
Circular polarization
λ_s=0.44; α_s=1.44
$dP(\lambda)/d\lambda^2>0$
STABILITY region
UNSTABLE region
P
λ
0
1
2
3
4
5
0.0
0.1
0.2
0.3
0.4
0.5
0.6

SOLITON DYNAMICS

Propagation of stable GNLS soliton

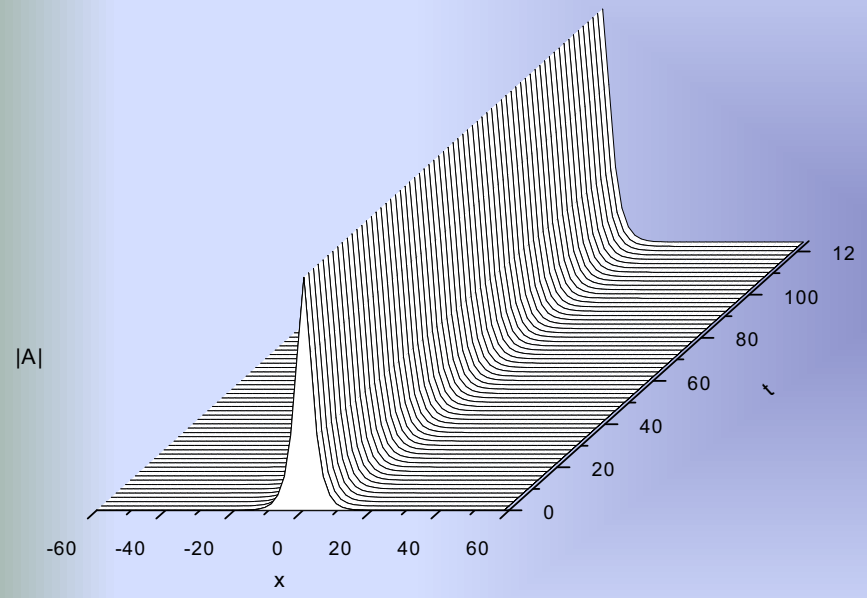

Propagation of unstable GNLS soliton

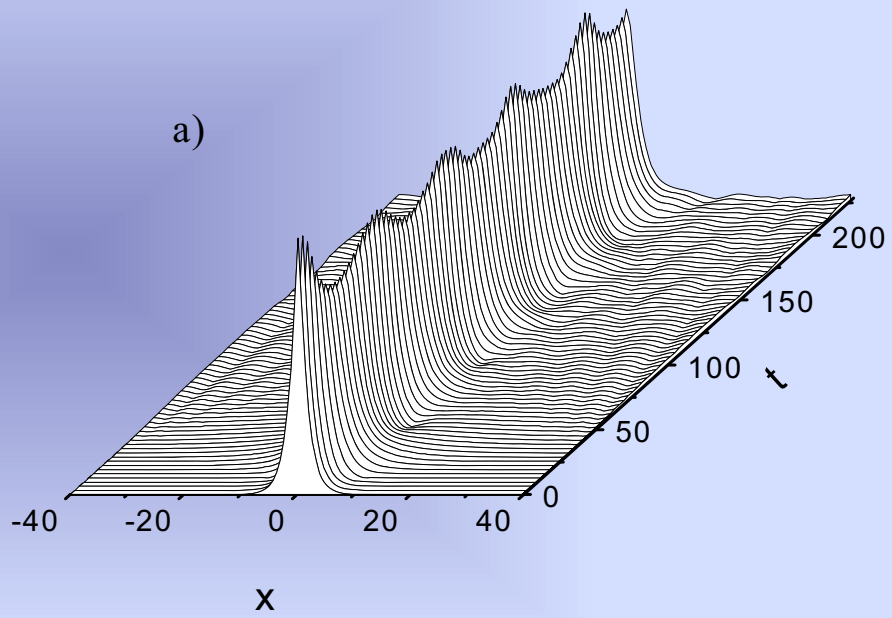

Fluid –Maxwell simulations

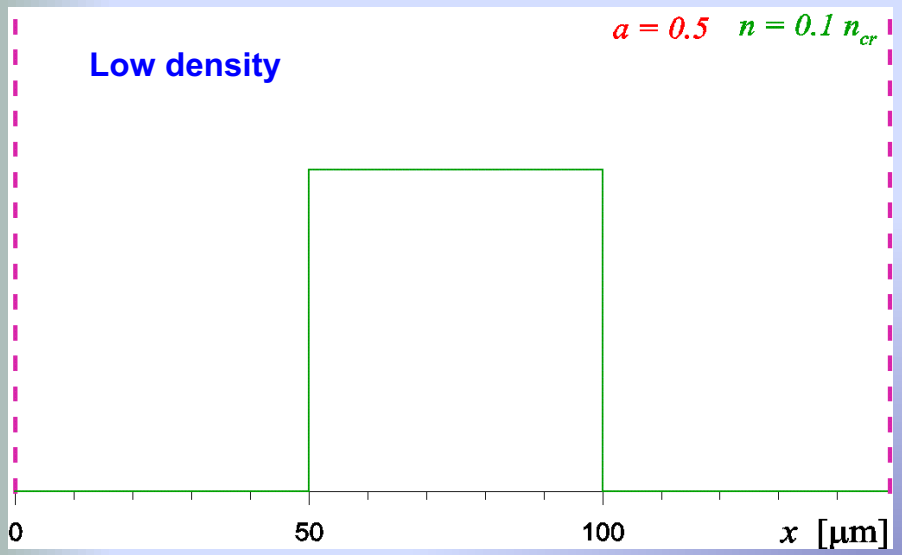

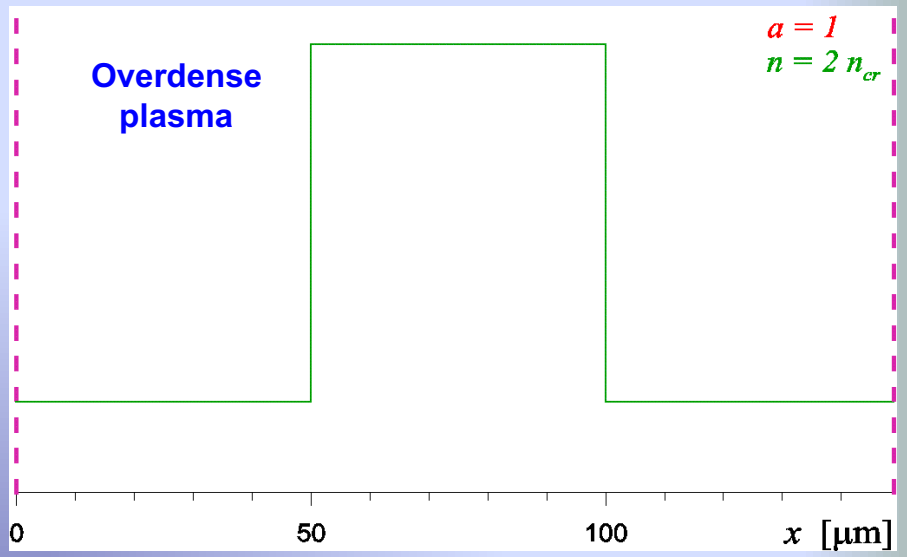

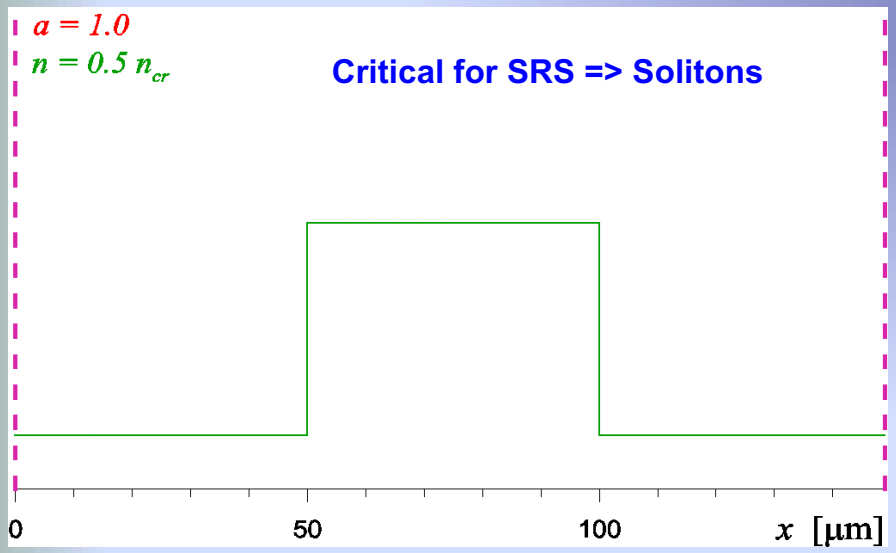

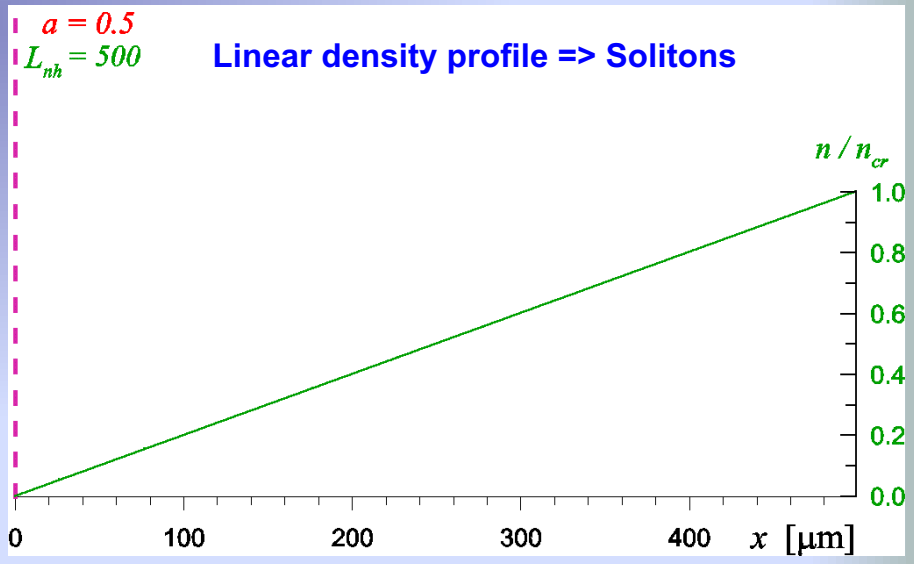

Method of particle simulations (Particle-In-Cell)

System represented by large number of (~ million) particles (electrons & ions)

Evolution of each particle (position, velocity) in self-consistent EM field is solved in time

$$\frac{d\vec{p}_k}{dt} = q\left(\vec{E} + \frac{1}{c}\vec{v}_k \times \vec{B}\right)$$

$$\frac{d\vec{x}_k}{dt} = \vec{v}_k$$

By summing up all effective charge and current densities necessary for calculating temporal values of local EM fields from Maxwell equations

$$\nabla \cdot \vec{E} = \sum_k q_k \delta(\vec{x} - \vec{x}_k)$$

$$\nabla \times \vec{B} = \frac{1}{c}\frac{\partial \vec{E}}{\partial t} + \frac{4\pi}{c}\sum_k q_k \vec{v}_k \delta(\vec{x} - \vec{x}_k)$$

Kinetic effects !

Landau damping
particle trapping …

Relativistic standing EM Soliton

(L=0.15mm, n_0=0.03 n_{cr}, T_e=1KeV)

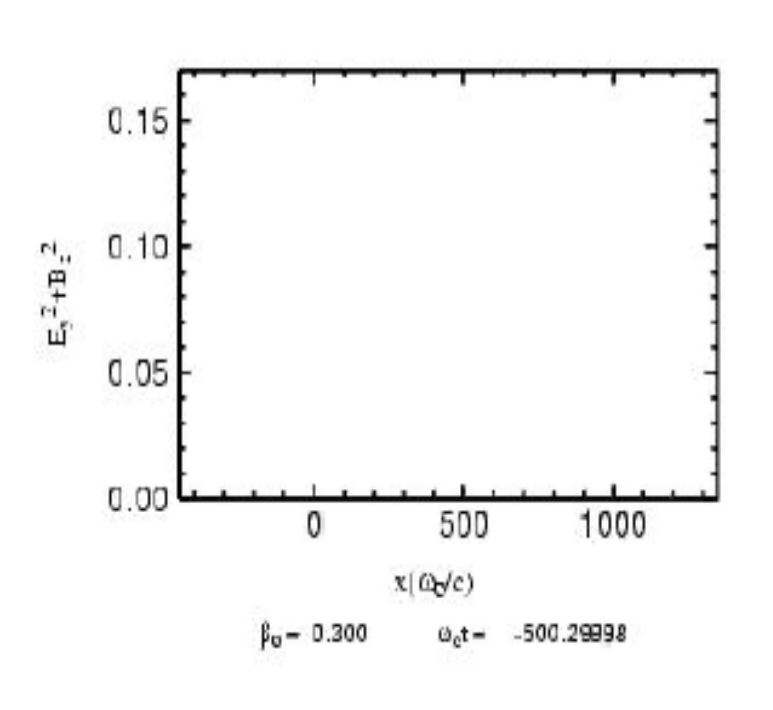

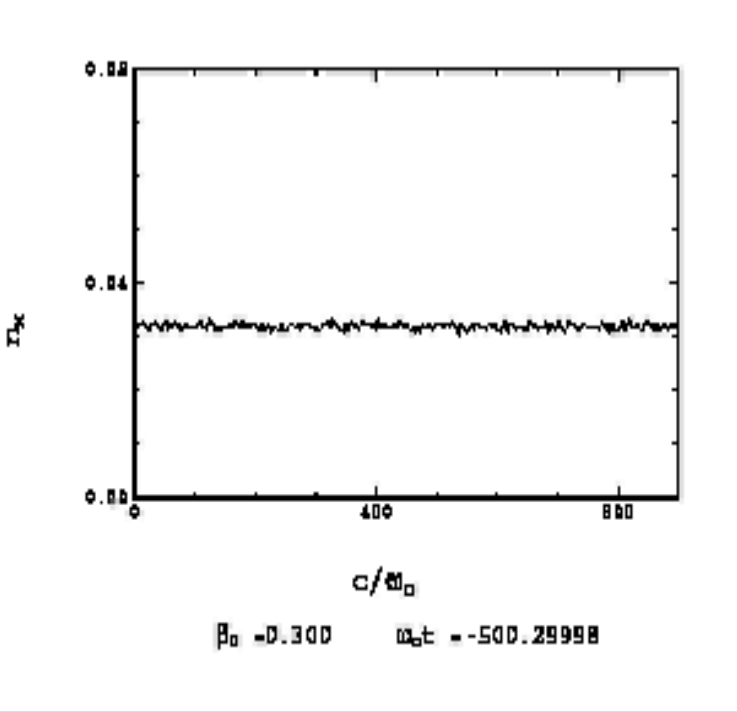

Laser fusion – Fast Ignition concept

Fast Ignition; attractive concept with high fusion gain by using Ultra-short High Intensity laser spark

Fast ignition: Compression and heating phases are separated

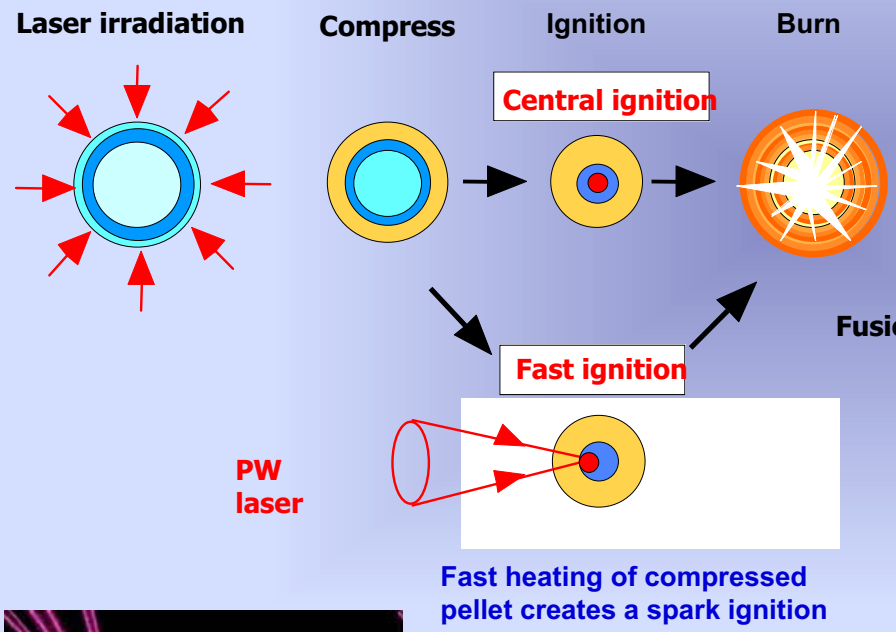

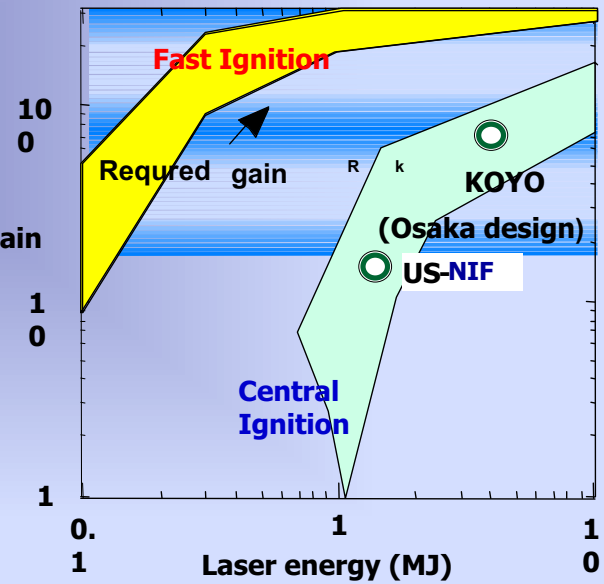

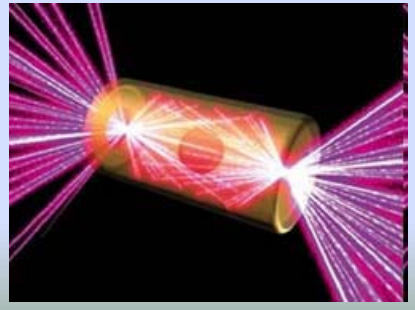

National Ignition Facility-NIF, Livermore
2-4 MJ in 192 laser beams (2009)

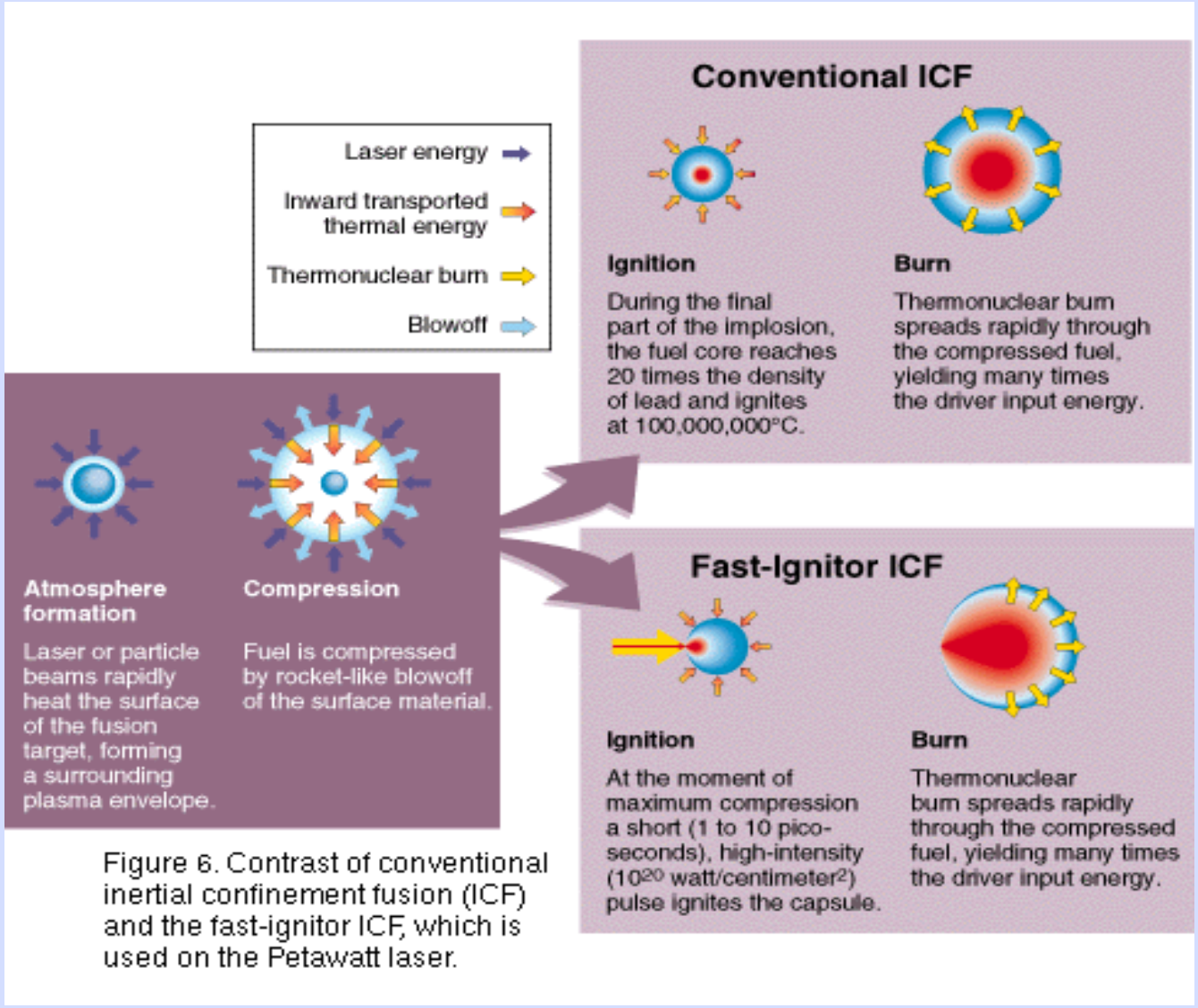

Figure 6. Contrast of conventional inertial confinement fusion (ICF) and the fast-ignitor ICF, which is used on the Petawatt laser.

ILE, Osaka has unique capability to conduct Fast Ignition model experiments -FIREX (2009)

ILE Osaka

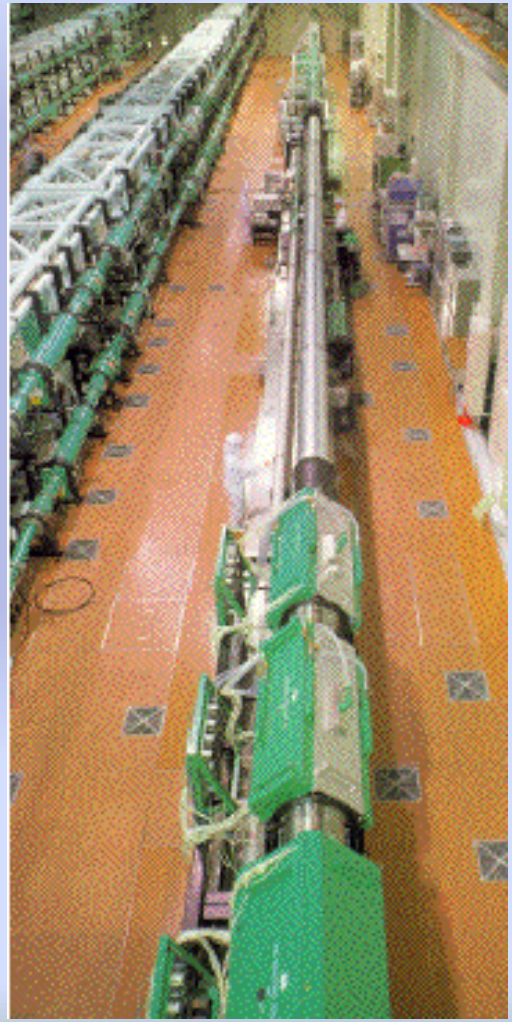

GEKKO laser: 12 green laser beams
E= 5 kJ, t = 1-2 nsec.
Uniform irradiation for high density compression.

PW laser: 1 beam
At 1 micron. (2005)
PW peak power is utilized for fast heating.

Laser technology for PW systems

Crossing the Petawatt Threshold

An extraordinarily powerful new laser promises to help make fusion power more easily attainable with "fast ignition." the laser beam's ultrashort pulses and extremely high intensities will also enable researchers to advance their understanding of the fundamental nature of energy and matter.

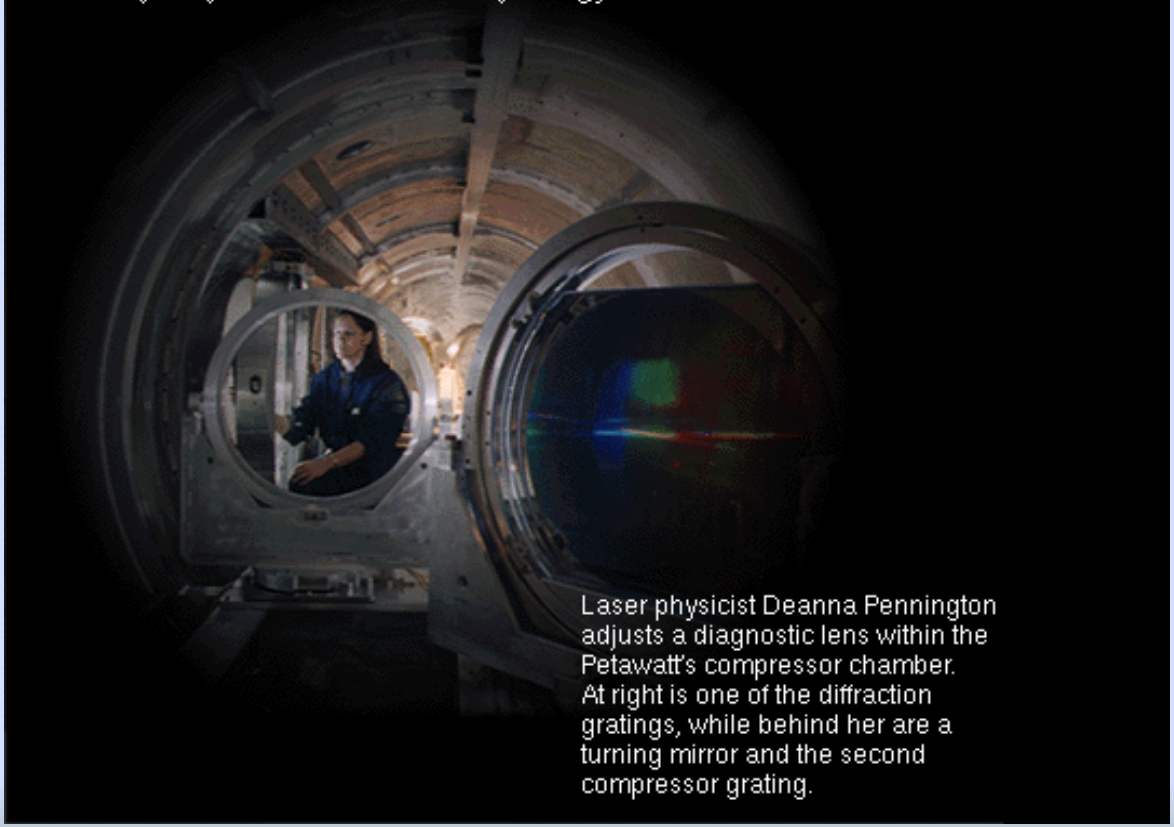

Laser physicist Deanna Pennington adjusts a diagnostic lens within the Petawatt's compressor chamber. At right is one of the diffraction gratings, while behind her are a turning mirror and the second compressor grating.

CCLRC Rutherford Appleton Laboratory

Pump requirements

Various applications of High-Field Plasma Science

Ultra High Intensity Ti:S = High Energy Pump

High Energy - many 10's Joules

Green wavelengths (~530 nm)

Can be "long" duration

Reasonable Repetition Rate

Reasonable Beam Quality

Low Cost

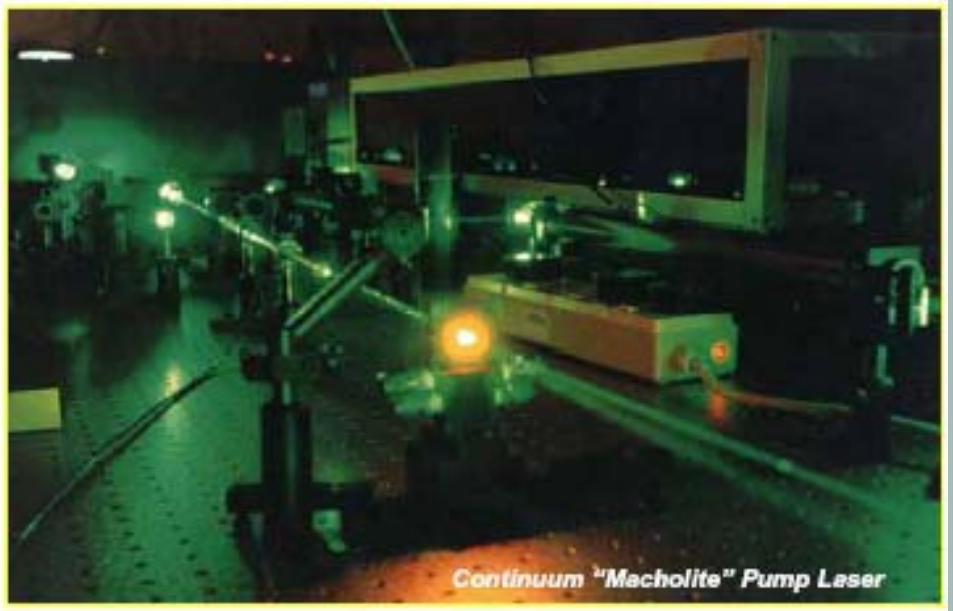

Continuum "Macholite" Pump Laser

X-ray image obtained from the point source by CPA laser-plasma

RADIOGRAPH OF A RAT shows the very high resolution that can be achieved by using x-rays generated from a tiny spot of plasma at the focus of a tabletop ultrahigh-intensity laser.

Laser Lightning Arrestor

Ultra-short CPA laser as a trigger

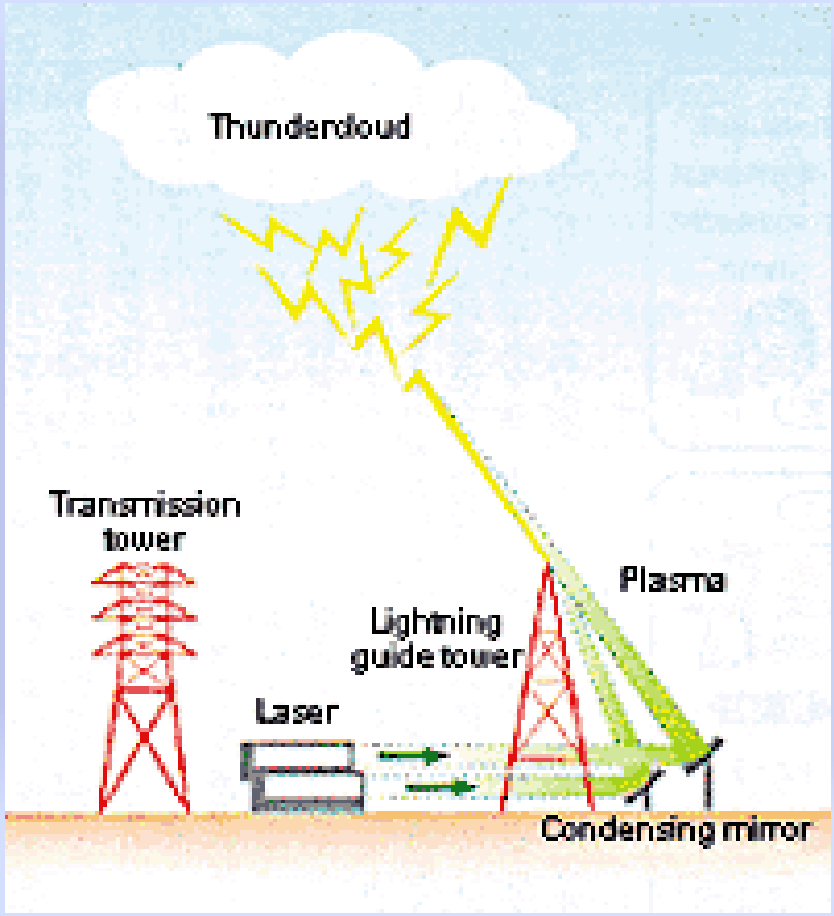

Light- laser bullets

Progress in high power laser. Very short (~ 100 fsec) laser pulses with powers of 100 TW.

Chirped Pulse Amplification Scheme

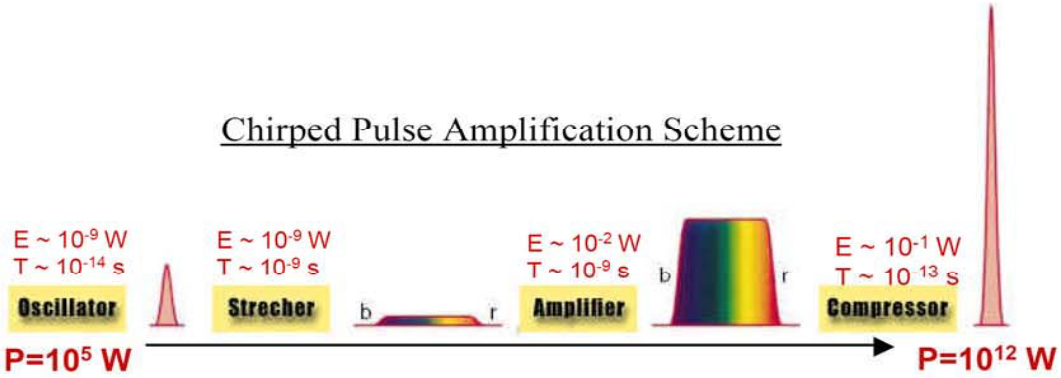

Propagation of these highly powered pulses in air leads to the collapse of the beam to "light bullets" (filaments) that can propagate for long distances. Inside the filaments the pulse under goes temporal and spectral changes.

"Light Bullets" – Filaments

$\lambda = 0.8\mu m$, $P = 2.2TW$, E = $240mJ$, $\tau = 110\, f$ sec

$10Hz\ rep-rate$, $L_{peak} = 2km$, $L_{\max} = 12km$, $\eta = 40\%$

* L. Woste, et al., Laser und Optoelektronik, **29**, 51 (1997)

Summary

- *Single electron dynamics => nonlinear, multi modal & multi-Dimensional*
- *Collective => relativistic plasma physics : nonlinear, multi-modal & multi-D*

for moderately relativistic laser-subcritical plasmas (A_0~1)

- *Electronic parametric instabilities strongly modified, broadened and merged*
- *Stimulated B- and F- Raman scattering dominate in underdense plasmas*
- *Novel relativistic SEAS versus SRS instability in subcritical plasma*
- *Coherence and turbulence; Raman cascade-into-condensate*
- *Raman complexity versus FS pulse generation and spectral features*
- *Strong turbulence and relativistic coherent EM localized structures*

Common features: Coherence versus turbulence

- *Relativistic plasma physics is "bifurcating" into two main branches*

- Laser fusion, high-energy densities and laboratory plasma astrophysics

- Ultra high field science, particle acceleration, atto-physics, nuclear physics

- *Many future challenges for experiments, theory and computer simulations*

References

- Skoric et al, LIRPP, vol 11, ed. by G. Miley, AIP (1994)
- Skoric et al. Phys. Rev E**53**, 4056(1996);ibid., E**60**, 7426 (1999)
- Jovanovic & Skoric, Physica Scripta (1997)
- Miyamoto, et al. J. Phys. Soc. Japan **67**, 1281 (1998)
- Skoric, et al. ICPIG 1999 (invited lecture); J. Tech. Phys. (2000)
- Mima, Skoric, et al Phys. Plasmas **8**, 2349 (2001)(ICPP-APS 2000)
- Hadzievski, Skoric, et al., Phys. Plasmas **9**, 2569 (2002)
- Nikolic, Skoric, Ishiguro & Sato, Phys. Rev. E**66**, 036404 (2002)
- Skoric et al, AIP Conf. Proc., Vol. **634**, pp. 99-106 (2002)
- Nikolic, Skoric, Ishiguro & Sato, Fusion Sci. & Tech. (2003)
- LiBaiwen, Ishiguro, Skoric & Sato, Laser & Part. Beams (2004)

Education and Training of Young Generation

at National Institute for Fusion Science, Japan

http://www.nifs.ac.jp

Graduate Course University

The Graduate University for Advanced Studies (SOKENDAI)

Cooperated Course with Nagoya Univ.

Acceptance of Graduate University Students

Summer School for Young Students

Asian Winter School

http://soukenweb.nifs.ac.jp/eindex.html

Plasma and Fusion Simulation Science
National Institute for Fusion Science
Toki, Japan

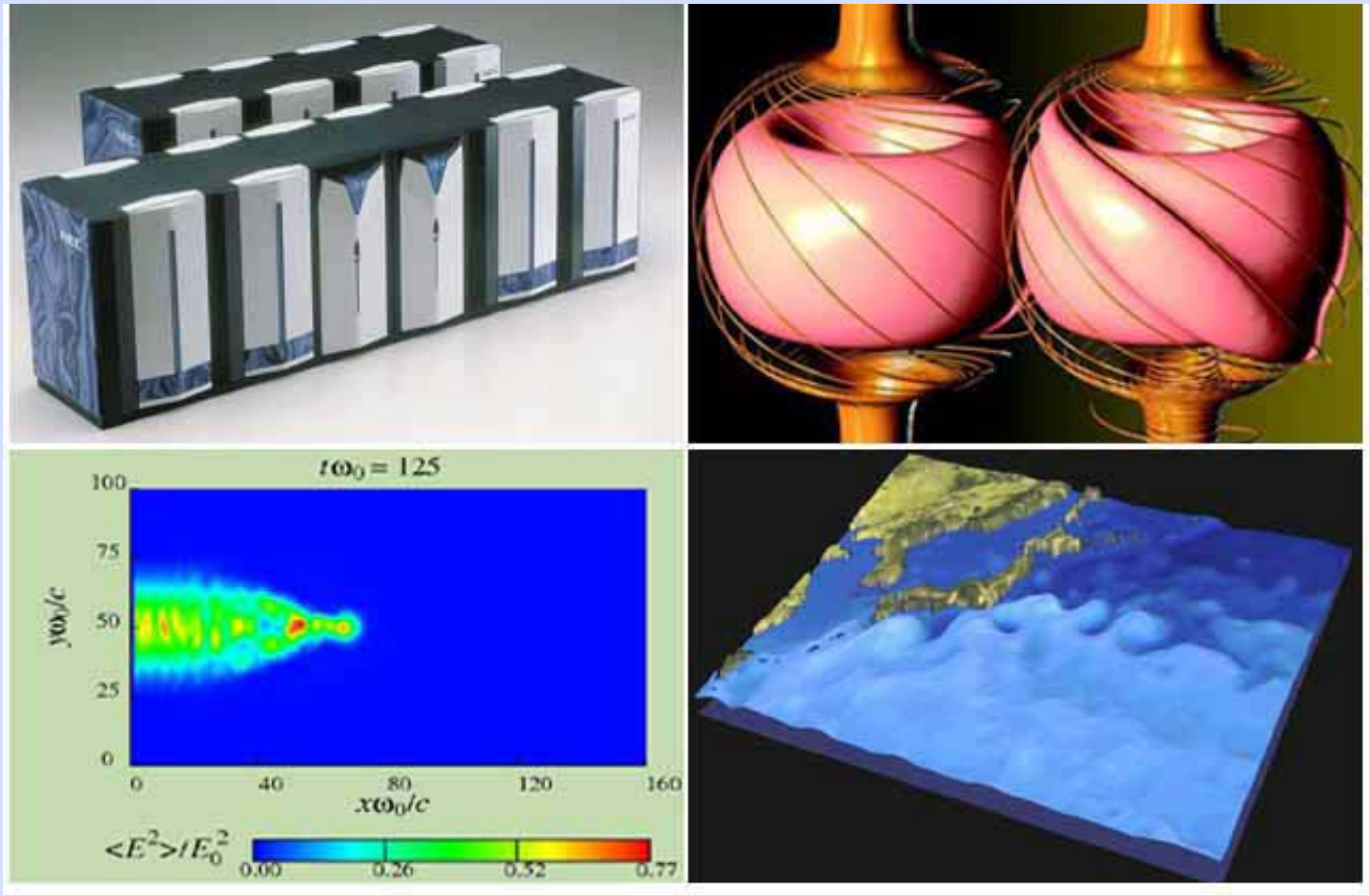

The Graduate University for Advanced Studies
School of Physical Sciences
Department of
Sokendai **Fusion Science**

http://soken.nifs.ac.jp/index.html

Thank you and see you …!?